e-ISSN 1308-8459

Official Publication of the Turkish Society of Anatomy and Clinical Anatomy

http://dergipark.org.tr/en/pub/anatomy

anatomy

An International Journal of Experimental and Clinical Anatomy

Volume 18 / Issue 3 / December 2024

Published three times a year

deomed®

https://dergipark.org.tr/tr/pub/anatomy

anatomy

An International Journal of Experimental and Clinical Anatomy

Official Publication of the Turkish Society of Anatomy and Clinical Anatomy

Aim and Scope

Anatomy, an international journal of experimental and clinical anatomy, is a peer-reviewed journal published three times a year with an objective to publish manuscripts with high scientific quality from all areas of anatomy. The journal offers a forum for anatomical investigations involving gross, histologic, developmental, neurological, radiological and clinical anatomy, and anatomy teaching methods and techniques. The journal is open to original papers covering a link between gross anatomy and areas related with clinical anatomy such as experimental and functional anatomy, neuroanatomy, comparative anatomy, modern imaging techniques, molecular biology, cell biology, embryology, morphological studies of veterinary discipline, and teaching anatomy. The journal is currently indexing and abstracting in TUBITAK ULAKBIM Turkish Medical Index, Proquest, EBSCO Host, Index Copernicus and Google Scholar.

Publication Ethics

Anatomy is committed to upholding the highest standards of publication ethics and observes the principles of Journal's Publication Ethics and Malpractice Statement which is based on the recommendations and guidelines for journal editors developed by the Committee on Publication Ethics (COPE), Council of Science Editors (CSE), World Association of Medical Editors (WAME) and International Committee of Medical Journal Editors (ICMJE). Fore detailed information please visit the online version of the journal which is available at https://dergipark.org.tr/tr/pub/anatomy

Authorship

All persons designated as authors should have participated sufficiently in the work to take public responsibility for the content of the manuscript. Authorship credit should be based on substantial contributions to (1) conception and design or analysis and interpretation of data, (2) drafting of the manuscript or revising it for important intellectual content and, (3) final approval of the version to be published. The Editor may require the authors to justify assignment of authorship. In the case of collective authorship, the key persons responsible for the article should be identified and others contributing to the work should be recognized with proper acknowledgment.

Copyright

Publisher

Deomed Publishing
Gür Sok. No:7/B Kadıköy, İstanbul, Türkiye
Phone: +90 216 414 83 43 (Pbx) / Fax: +90 216 414 83 42
www.deomed.com / e-mail: medya@deomed.com

deomed®

Publication Information

Anatomy (e-ISSN 1308-8459) as an open access electronic journal is published by Deomed Publishing, Istanbul, for the Turkish Society of Anatomy and Clinical Anatomy, TSACA. Due the Press Law of Turkish Republic dated as June 26, 2004 and numbered as 5187, this publication is classified as a periodical in English language.

Ownership
On behalf of the Turkish Society of Anatomy and Clinical Anatomy,
Ahmet Kağan Karabulut, MD, PhD; Konya, Türkiye

Editor-in-Chief
Nihal Apaydın, MD
Department of Anatomy,
Faculty of Medicine, Ankara University,
06100, Sıhhıye, Ankara, Türkiye
Phone: 0090 312 595 82 48
e-mail: napaydin@gmail.com; napaydin@medicine.ankara.edu.tr

Administrative Office
Güven Mah. Güvenlik Cad. Onlar Ap. 129/2 Aşağı Ayrancı, Ankara, Türkiye
Phone: +90 312 447 55 52-53

Submission of Manuscripts

Manuscripts should be submitted at our manuscript submission and information portal https://dergipark.org.tr/en/pub/anatomy

Categories of Articles

- ***Original Articles*** describe substantial original research that falls within the scope of the Journal.
- ***Teaching Anatomy*** section contains regular or all formats of papers which are relevant to comparing teaching models or to introducing novel techniques, including especially the own experiences of the authors.
- ***Reviews*** section highlights current development in relevant areas of anatomy. The reviews are generally invited; other prospective authors should consult with the Editor-in-Chief.
- ***Case Reports*** include new, noteworthy or unusual cases which could be of help for basic notions and clinical practice.
- ***Technical Note*** articles cover technical innovations and developments with a specific technique or procedure or a modification of an existing technique. They should be sectioned like an original research article but not exceed 2000 words.
- ***Viewpoint*** articles give opinions on controversial topics or future projections, some of these are invited.
- ***Historical View*** category presents overview articles about historical sections from all areas of anatomy.
- ***Terminology Zone*** category is a platform for the articles which discuss some terminological controversies or opinions.

The categories above are peer-reviewed. They should include abstract and keywords. There are also categories including Letters to the Editor, Book Reviews, Abstracts, Obituary, News and Announcements which do not require a peer review process.

For detailed instructions concerning the submission of manuscripts, please refer to the Instructions to Authors.

Advertising and Reprint Requests

Please direct to publisher. e-mail: medya@deomed.com

Instructions to Authors

Anatomy, an international journal of experimental and clinical anatomy, is the official publication of the Turkish Society of Anatomy and Clinical Anatomy, TSACA. It is a peer-reviewed e-journal that publishes scientific articles in English. For a manuscript to be published in the journal, it should not be published previously in another journal or as full text in congress books and should be found relevant by the editorial board. Also, manuscripts submitted to Anatomy must not be under consideration by any other journal. Relevant manuscripts undergo conventional peer review procedure (at least three reviewers). For the publication of accepted manuscripts, author(s) should reveal to the Editor-in-Chief any conflict of interest and transfer the copyright to the Turkish Society of Anatomy and Clinical Anatomy, TSACA.

In the Materials and Methods section of the manuscripts where experimental studies on humans are presented, a statement that informed consent was obtained from each volunteer or patient after explanation of the procedures should be included. This section also should contain a statement that the investigation conforms with the principles outlined in the appropriate version of 1964 Declaration of Helsinki. For studies involving animals, all work must have been conducted according to applicable national and international guidelines. Prior approval must have been obtained for all protocols from the relevant author's institutional or other appropriate ethics committee, and the institution name and permit numbers must be provided at submission.

Anatomical terms used should comply with Terminologia Anatomica by FCAT (1998).

No publication cost is charged for the manuscripts but reprints and color printings are at authors' cost.

Preparation of manuscripts

During the preparation of the manuscripts, uniform requirements of the International Committee of Medical Journal Editors, a part of which is stated below, are valid (*see* ICMJE. Uniform requirements for manuscripts submitted to biomedical journals. Updated content is available at www.icmje.org). The manuscript should be typed double-spaced on one side of a 21×29.7 cm (A4) blank sheet of paper. At the top, bottom and right and left sides of the pages a space of 2.5 cm should be left and all the pages should be numbered except for the title page.

Manuscripts should not exceed 15 pages (except for the title page). They must be accompanied by a cover letter signed by corresponding author and the Conflicts of Interest Disclosure Statement and Copyright Transfer Form signed by all authors. The contents of the manuscript (original articles and articles for Teaching Anatomy category) should include: 1- Title Page, 2- Abstract and Keywords, 3- Introduction, 4- Materials and Methods, 5- Results, 6- Discussion (Conclusion and/or Acknowledgement if necessary), 7- References

Title page

In all manuscripts the title of the manuscript should be written at the top and the full names and surnames and titles of the authors beneath. These should be followed with the affiliation of the author. Manuscripts with long titles are better accompanied underneath by a short version (maximum 80 characters) to be published as running head. In the title page the correspondence address and telephone, fax and e-mail should be written. At the bottom of this page, if present, funding sources supporting the work should be written with full names of all funding organizations and grant numbers. It should also be indicated in a separate line if the study has already been presented in a congress or likewise scientific meeting. Other information such as name and affiliation are not to be indicated in pages other than the title page.

Abstract

Abstract should be written after the title in 100–250 words. In original articles and articles prepared in IMRAD format for Teaching Anatomy category the abstract should be structured under sections Objectives, Methods, Results and Conclusion. Following the abstract at least 3 keywords should be added in alphabetical order separated by semicolumns.

References

Authors should provide direct references to original research sources. References should be numbered consecutively in square brackets, according to the order in which they are first mentioned in the manuscript. They should follow the standards detailed in the NLM's Citing Medicine, 2nd edition (Citing medicine: the NLM style guide for authors, editors, and publishers [Internet]. 2nd edition. Updated content is available at www.ncbi.nlm .nih.gov/books/NBK7256). The names of all contributing authors should be listed, and should be in the order they appear in the original reference. The author is responsible for the accuracy and completeness of references. When necessary, a copy of a referred article can be requested from the author. Journal names should be abbreviated as in *Index Medicus*. Examples of main reference types are shown below:

- **Journal articles:** Author's name(s), article title, journal title (abbreviated), year of publication, volume number, inclusive pages
  - *Standard journal article:* Sargon MF, Celik HH, Aksit MD, Karaagaoglu E. Quantitative analysis of myelinated axons of corpus callosum in the human brain. Int J Neurosci 2007;117:749–55.
  - *Journal article with indication article published electronically before print:* Sengul G, Fu Y, Yu Y, Paxinos G. Spinal cord projections to the cerebellum in the mouse. Brain Struct Funct Epub 2014 Jul 10. DOI 10.1007/s00429-014-0840-7.
- **Books:** Author's name(s), book title, place of publication, publisher, year of publication, total pages (entire book) or inclusive pages (contribution to a book or chapter in a book)
  - *Entire book:*
    - *Standard entire book:* Sengul G, Watson C, Tanaka I, Paxinos G. Atlas of the spinal cord of the rat, mouse, marmoset, rhesus and human. San Diego (CA): Academic Press Elsevier; 2013. 360 p.
    - *Book with organization as author:* Federative Committee of Anatomical Terminology (FCAT). Terminologia anatomica. Stuttgart: Thieme; 1998. 292 p.
    - *Citation to a book on the Internet:* Bergman RA, Afifi AK, Miyauchi R. Illustrated encyclopedia of human anatomic variation. Opus I: muscular system [Internet]. [Revised on March 24, 2015] Available from: http://www.anatomyatlases.org/AnatomicVariants/AnatomyHP.shtml
  - *Contribution to a book:*
    - *Standard reference to a contributed chapter:* Potten CS, Wilson JW. Development of epithelial stem cell concepts. In: Lanza R, Gearhart J, Blau H, Melton D, Moore M, Pedersen R, Thomson J, West M, editors. Handbook of stem cell. Vol. 2, Adult and fetal. Amsterdam: Elsevier; 2004. p. 1–11.
    - *Contributed section with editors:* Johnson D, Ellis H, Collins P, editors. Pectoral girdle and upper limb. In: Standring S, editor. Gray's anatomy: the anatomical basis of clinical practice. 29th ed. Edinburgh (Scotland): Elsevier Churchill Livingstone; 2005. p. 799–942.
  - *Chapter in a book:*
    - *Standard chapter in a book:* Doyle JR, Botte MJ. Surgical anatomy of the hand and upper extremity. Philadelphia (PA): Lippincott Williams and Wilkins; 2003. Chapter 10, Hand, Part 1, Palmar hand; p. 532–641.

Illustrations and tables

Illustrations and tables should be numbered in different categories in the manuscript and Roman numbers should not to be used in numbering. Legends of the illustrations and tables should be added to the end of the manuscript as a separate page. Attention should be paid to the dimensions of the photographs to be proportional with 10x15 cm. Some abbreviations out of standards can be used in related illustrations and tables. In this case, abbreviation used should be explained in the legend. Figures and tables published previously can only be used when necessary for a comparison and only by giving reference after obtaining permission from the author(s) or the publisher (copyright holder).

Author Contribution

Each manuscript should contain a statement about the authors' contribution to the Manuscript. Please note that authorship changes are no longer possible after the final acceptance of an article.

List each author by the initials of names and surnames and describe each of their contributions to the manuscript using the following terms:

- Protocol/project development
- Data collection or management
- Data analysis
- Manuscript writing/editing
- Other (please specify briefly using 1 to 5 words)

For example: NBA: Project development, data collection; AS: Data collection, manuscript writing; STR: Manuscript writing

Funding: information that explains whether and by whom the research was supported.

Conflicts of interest/Competing interests: include appropriate disclosures.

Ethics approval: include appropriate approvals or waivers. Submitting the official ethics approval by whom the research was approved, including the approval date, number or code is necessary.

If the submission uses cadaveric tissue, please acknowledge the donors in an acknowledgement at the end of the paper.

Control list

- Length of the manuscript (max. 15 pages)
- Manuscript format (double space; one space before punctuation marks except for apostrophes)
- Title page (author names and affiliations; running head; correspondence)
- Abstract (100–250 words)
- Keywords (at least three)
- References (relevant to *Index Medicus)*
- Illustrations and tables (numbering; legends)
- Conflicts of Interest Disclosure Statement and Copyright Transfer Form
- Cover letter

All manuscripts must contain the following declaration sections. These should be placed before the reference list at the end of the manuscript.

Original Article

http://dergipark.org.tr/en/pub/anatomy
Received: May 6, 2024; Accepted: October 23, 2024
doi:10.2399/ana.24.1479104

anatomy
http://dergipark.org.tr/en/pub/anatomy
An International Journal of Experimental and Clinical Anatomy

Fetal anatomy of the abductor pollicis brevis and its clinical importance

Saliha Seda Adanır[1], Simge Korkmaz[2], Orhan Beger[1], İlhan Bahşi[1], Piraye Kervancıoğlu[1], Mustafa Orhan[1]

[1]*Department of Anatomy, Faculty of Medicine, Gaziantep University, Gaziantep, Türkiye*
[2]*Faculty of Medicine, Gaziantep University, Gaziantep, Türkiye*

Abstract

Objectives: The abductor pollicis brevis exhibits a variant course in newborns with radial polydactyly or syndactyly; however, its morphology in human fetuses has not been previously studied. This study aims to document the dimensions and attachment points of abductor pollicis brevis in human fetuses.

Methods: The study consisted of 27 (15 females and 12 males) fetuses with a mean gestational age of 24.08±4.18 weeks. The attachment points (its insertion and origin) of abductor pollicis brevis were determined. The width, length and area of the muscle were measured with ImageJ software. The insertion and origin points were classified according to the literature.

Results: The mean width, length and area of abductor pollicis brevis were 3.52±1.33 mm, 9.19±2.73 mm and 30.84±20.39 mm^2, respectively. The muscle most commonly originated from the flexor retinaculum and the tubercle of the scaphoid bone (Type 1) and inserted at the lateral side of the first metacarpophalangeal joint (Type A).

Conclusion: This study is the first to classify the origin and insertion of the abductor pollicis brevis in human fetuses. These findings could be valuable for hand surgeons performing surgical interventions in this region in newborns. Additionally, the growth patterns identified in our study may be used to estimate the size of the abductor pollicis brevis in fetuses.

Keywords: abductor pollicis brevis; fetus; thenar region; thumb

Anatomy 2024;18(3):73–82 ©2024 Turkish Society of Anatomy and Clinical Anatomy (TSACA)

Introduction

The thenar region muscles play a crucial role in thumb strength and movement, and they are closely associated with anomalies and surgical procedures in this area. One of the thenar muscles, the abductor pollicis brevis (APB), is a slender muscle located at the proximal and lateral part of the thenar eminence. The muscle primarily originates from the flexor retinaculum, with additional fibers arising from the tendon of the abductor pollicis longus and the scaphoid tubercle. It attaches to the base of the proximal phalanx.[1] Variations related to the APB, such as the absence of the muscle, double-headed muscle, fusion with the abductor pollicis longus, or attachment to other thenar muscles, have been documented in the literature.[2]

Thenar muscle agenesis can occur in cases of thumb hypoplasia.[3] During thumb anomalies like syndactyly and radial polydactyly—conditions that are sensitive in pediatric surgery both aesthetically and functionally—the APB may deviate from its normal course in newborns. Atrophy or hypoplasia of this muscle, whether occurring before or after syndactyly and polydactyly surgery, underscores the importance of understanding the normal developmental and morphometric characteristics of the muscle.[4–8] However, a fetal study on the anatomical features of the APB has not been reported in the literature. Furthermore, no previous classification exists regarding the origin and insertion of the APB. In this context, this study aims to establish new classifications based on the origin and insertion of the APB and to examine its morphometric features in human fetuses to inform early childhood surgeries.

This study was presented as an oral presentation at the 20th IFAA Congress held from August 5–7, 2022.

Materials and Methods

This study was conducted in accordance with the ethical standards outlined in the 1964 Declaration of Helsinki and its subsequent amendments. The thenar regions of 27 fetuses (12 males, 15 females) with a mean gestational age of 24.08±4.18 (range: 18–35) weeks which had been fixed in 10% formalin, were dissected bilaterally. Fetal age was determined based on foot length, as detailed in **Table 1**.[9] Fetuses with deformities such as polydactyly, syndactyly, or cleft lip were excluded from the study.

The dissections were carried out in the university's anatomy department. Fetal samples were placed in the supine position with their hands open. Using a surgical microscope (Leica S4E; Leica Microsystems GmbH, Wetzlar, Germany) the skin and fasciae were carefully dissected. These structures were then retracted laterally and/or medially to expose the APB muscle.

The thumbs were photographed in standard position using a 64 MP camera (Apple iPhone 13 mobile device, running the iOS 14.2.1 operating system) with x10 digital magnification. Measurements were taken three times by two independent observers from the photographs using a digital image analysis program (ImageJ; US National Institutes of Health, Bethesda, USA). The following parameters were measured (**Figure 1**):

- **APB-L (mm):** the length of APB (the distance between the origin and insertion of the muscle) (**Figure 1a**)
- **APB-W (mm):** the width of APB (the width at the widest part of the muscle) (**Figure 1b**)
- **APB-A (mm^2):** the area of APB (the area measured by drawing the boundaries of the muscle) (**Figure 1c**)

Previous studies related to variations of the origin of APB were searched in PubMed and Google Scholar databases, and a classification was developed to encompass all identified variations. Articles lacking detailed information on these variations were excluded based on the following criteria: absence of data about sides, non-English language articles, and articles with only an abstract. The literature search was conducted using the following keywords: "abductor pollicis brevis," "abductor pollicis brevis and origin," and "abductor pollicis brevis and variation." As a result of this search, 178 studies were included in our classification, leading to the division of the origin of the APB into seven types (**Table 2**).

Similarly, studies related to variations in the insertion of the APB were searched in the PubMed and Google Scholar databases. Articles without detailed information on variations were excluded using the same criteria: absence of data about sides, non-English language articles, and articles with only an abstract. The keywords used for this literature review were: "abductor pollicis brevis", "abductor pollicis brevis and insertion", and "abductor pollicis brevis and variation." Following this search, 178 studies were included in our classification, and the insertion of the APB was categorized into four types (**Table 3**).

Table 1
Demographic data of fetuses.

Month	Gestational week	N	Length of right foot (mm)	Males (n)	Females (n)
V	18	1	27.12	0	1
	19	2	29.34±0.50	1	1
VI	21	3	33.16±1.38	2	1
	22	3	37.01±1.54	1	2
	23	2	40.40±0.55	0	2
	24	2	42.12±1.85	0	2
VII	25	2	44.19±0.57	2	0
	26	1	45.25	0	1
	27	3	49.66±1.03	1	2
	28	2	51.97±0.04	1	1
VIII	29	1	54.75	1	0
	32	1	59.08	1	0
IX	35	1	62.86	0	1
Total	24.08±4.18	27	41.38±9.83	12	15

N, n: number of fetuses.

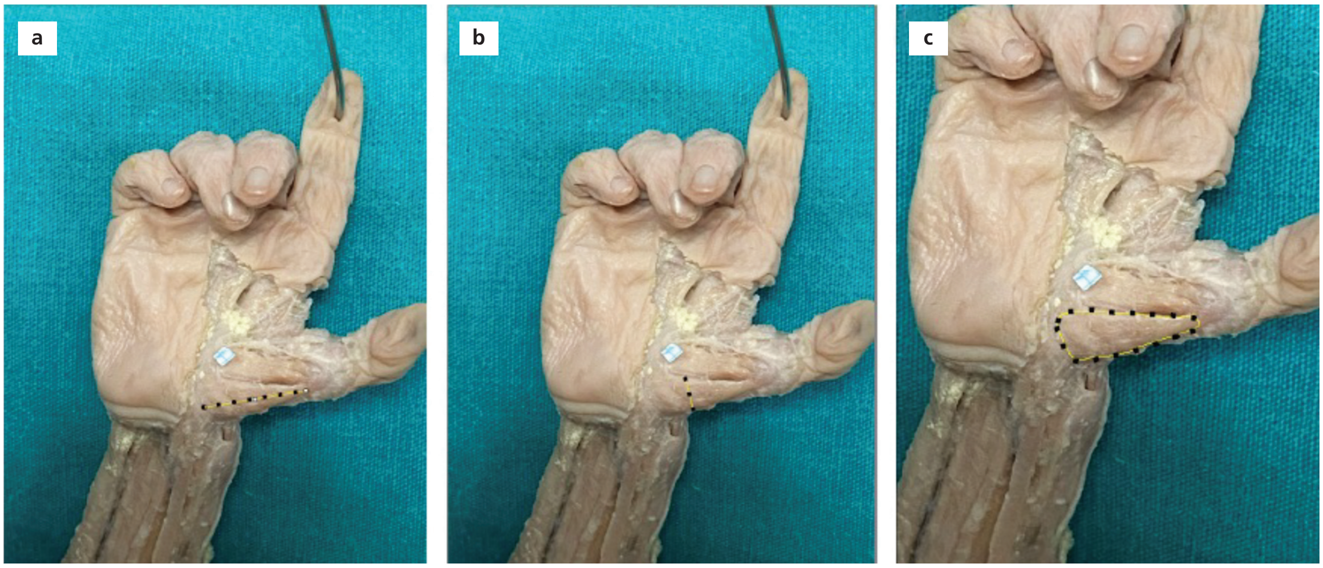

Figure 1. Measurements of length (**a**), width (**b**) and area (**c**) of abductor pollicis brevis.

Intra-observer and inter-observer evaluations were conducted to test the reliability of the measurements. Two researchers independently measured the parameters three times in total. The first observer (SSA) performed the measurements twice, while the second observer (SK) conducted the measurements once. The mean values were calculated by averaging these three measurements. A paired samples t-test was used to compare the two measurements made by SSA, and the intraclass correlation coefficient (ICC) was calculated to compare the measurements taken by SSA (first measurement) and SK.

Changes in the measured parameters according to gestational weeks and months were analyzed using one-way ANOVA followed by a post-hoc Bonferroni test. An inde-

Table 2
Description of types related to the origin of APB in the literature.

Type	Descriptions of types (attachment sites)	n (%)
1	Tubercle of scaphoid bone, flexor retinaculum	44 (84.62)
2	Flexor retinaculum	6 (11.54)
3	Tendon of abductor pollicis longus	2 (3.84)
4	Scaphoid bone	0
5	Flexor retinaculum and distal part of the fibrous sheath of the flexor carpi radialis tendon	0
6	Tendon of the palmaris longus	0
7	Absence of APB	0

Table 3
Description of types related to the insertion of APB in the literature.

Type	Descriptions of types (attachment sites)	n (%)
A	Lateral side of first metacarpophalangeal joint	40 (76.92)
B	Distal and lateral side of first metacarpal bone	9 (17.31)
C	Lateral side of first proximal phalanx	3 (5.77)
D	Absence of APB	0

Table 4
Comparison of the measured parameters in terms of sex and side.

Parameters	Sex			Side		
	Male (20 sides/40%)	Female (30 sides/60%)	p-value	Right	Left	p-value
APB-L (mm)	9.89±3.10	8.82±2.48	0.191	9.56±2.64	8.84±2.79	0.359
APB-W (mm)	3.83±1.53	3.35±1.20	0.228	3.51±1.19	3.51±1.47	0.991
APB-A (mm^2)	37.46±24.77	27.43±17.14	0.100	30.59±18.48	31.07±22.36	0.934

APB-A: area of abductor pollicis; **APB-L:** length of abductor pollicis brevis; **APB-W:** width of abductor pollicis brevis.

pendent samples t-test was used to compare male and female measurements, while a paired samples t-test was employed for right-left comparisons. The Pearson correlation coefficient was used to assess the relationships between the measured parameters. Simple linear regression analysis was applied to derive regression formulas for the measured parameters. Statistical analysis was performed using the SPSS for Windows, version 22.0 (IBM, Armonk, NY, USA), and a p-value of <0.05 was considered statistically significant.

Results

No statistically significant differences were observed in the measurements performed by the same investigator. Additionally, the intraclass correlation coefficient (ICC) score (ICC= 90%–98.6%) indicated that the reliability of the measurements was excellent. Measurements could not be clearly performed on four hands; therefore, the analysis was completed on 50 hands. The origin and insertion of the muscle could not be clearly defined on two hands, so these aspects were defined on only 52 sides. Side and sex comparisons of the measured parameters are presented in **Table 4**, which shows that the parameters did not differ based on side or sex. Growth patterns of the parameters relative to gestational weeks and months are provided in **Tables 5** and **6**, indicating that the parameters increased significantly with fetal age. Additionally, the parameters exhibited a significant positive correlation with each other (p<0.05).

Table 5
Growth patterns of the parameters according to gestational weeks.

Gestational week	APB–L (mm)	APB–W (mm)	APB–A (mm^2)
	Mean±SD (min–max)	Mean±SD (min–max)	Mean±SD (min–max)
18	7.31±2.85 (5.29–9.32)	2.60±0.51 (2.24–2.96)	16.44±7.47 (11.16–21.72)
19	7.25±0.85 (6.44–8.13)	2.42±0.77 (1.76–3.27)	15.79±6.38 (11.79–23.15)
20	6.57±1.09 (5.12–8.14)	2.19±0.17 (2.05–2.51)	13.00±1.94 (10.10–15.28)
21	7.71±1.40 (6.21–9.40)	2.60±0.20 (2.26–2.80)	19.24±1.67 (17.54–20.99)
22	7.70±0.96 (5.99–8.88)	3.62±0.53 (3.11–4.31)	24.97±4.60 (19.40–31.86)
23	7.91±0.57 (7.44–8.63)	2.90±0.39 (2.33–3.15)	19.47±1.57 (17.95–21.64)
24	11.72±4.15 (7.78–16.13)	4.10±1.14 (3.37–5.79)	48.11±33.46 (21.23–95.19)
25	9.46±1.50 (8.05–11.03)	3.46±0.55 (2.85–3.93)	28.48±8.40 (19.61–36.32)
26	7.84±1.51 (6.77–8.91)	2.01±0.76 (1.47–2.54)	12.77±8.00 (7.11–18.43)
27	10.59±1.63 (8.94–13.14)	3.92±0.82 (3.37–5.29)	36.38±9.54 (26.14–47.01)
28	11.36±1.15 (10.26–12.63)	4.32±0.42 (3.84–4.81)	44.20±6.40 (38.93–53.53)
29	12.02±1.22 (11.16–12.88)	5.64±0.25 (5.46–5.82)	68.75±8.29 (62.88–74.61)
32	15.81±0.03 (15.79–15.83)	6.19±0.49 (5.84–6.54)	80.92±0.57 (80.52–81.32)
35	11.15±0.82 (10.57–11.73)	6.30±2.21 (4.73–7.86)	49.30±16.24 (37.81–60.78)
Total	9.19±2.73 (5.12–16.13)	3.52±1.33 (1.47–7.86)	30.84±20.39 (7.11–95.19)
p-value	0.001	0.001	0.001

APB-A: area of abductor pollicis; **APB-L:** length of abductor pollicis brevis; **APB-W:** width of abductor pollicis brevis.

Table 6
Growth patterns of the parameters according to gestational months.

Month	APB-L (mm)	APB-W (mm)	APB-A (mm^2)
	Mean±SD (min–max)	Mean±SD (min–max)	Mean±SD (min–max)
5th	6.89±1.30 (5.12-9.32)	2.33±0.43 (1.76-3.27)	14.39±4.26 (10.10-23.15)
6th	8.59±2.53 (5.99-16.13)	3.30±0.82 (2.26-5.79)	27.17±17.98 (17.54-95.19)
7th	10.17±1.76 (6.77-13.14)	3.66±0.96 (1.47-5.29)	33.55±12.79 (7.11-53.53)
8th	13.92±2.30 (11.16-15.83)	5.92±0.45 (5.46-6.54)	74.83±8.51 (62.88-81.32)
9th	11.15±0.82 (10.57-11.73)	6.30±2.21 (4.73-7.86)	49.30±16.24 (37.81-60.78)
p-value	0.001	0.001	0.001

APB-A: area of abductor pollicis; **APB-L:** length of abductor pollicis brevis; **APB-W:** width of abductor pollicis brevis.

Based on our literature review and dissections, the origin of the APB was classified into seven types (**Table 7**). In this study, we identified three different types related to the origin of the APB (**Figure 2**). Type 1 was the most common, observed in 44 sides (84.62%) (right: 23, left: 21; male: 17, female: 27). Type 2 was detected in six sides (11.54%) (right: 2, left: 4; male: 2, female: 4). Type 3 was the least common, found in two sides (3.84%) (right: 1, left: 1; male: 1, female: 0).

Based on our literature review and dissections the insertion of APB was classified into four types (**Table 8**). In this study, we identified three different types related to the insertion of the APB (**Figure 3**). Type A was the most common, observed in 40 sides (76.92%) (right: 20, left: 20, male: 17, female: 23). Type B was detected in nine sides (17.31%) (right: 4, left: 5, male: 4, female: 5). Type C was the least common, found in in three sides (5.77%) (right: 2, left: 1, male: 1, female: 2).

The linear function for APB length (APB-L) was calculated as $y=-1.738+0.454 \times$ weeks ($p<0.001$), for APB width (APB-W) as $y=-2.449+0.248 \times$ weeks ($p<0.001$), and for APB area (APB-A) as $y=-51.342+3.413 \times$ weeks ($p<0.001$) (**Figure 4**).

Discussion

Previous studies showed that developmental anomalies in the hand or forearm occur in approximately one in 600 newborns[1] and congenital muscle diseases have an estimated prevalence of 4.7 per 100,000 newborns.[10] The most crucial period for the development of hand anomalies is between 12 and 16 weeks of gestation.[1] During early human development, limb formation begins with the establishment of the limb's foundation within the somatopleure of the lateral plate mesoderm. This foundation typically forms around the 24th day after conception, with the initial emergence of upper limb projections occurring in the lower cervical area. Following the formation of the limb foundation, three interconnected signaling hubs regulate the spatial arrangement of the limb in three dimensions. The primary signaling hub controls the expansion of the limb from the shoulder to the hand. The second hub, known

Table 7
Description of types related to the origin of APB in the literature .

Type	Descriptions of types (attachment sites)	n (%)
1	Tubercle of scaphoid bone, flexor retinaculum	44 (84.62)
2	Flexor retinaculum	6 (11.54)
3	Tendon of abductor pollicis longus	2 (3.84)
4	Scaphoid bone	0
5	Flexor retinaculum and distal part of the fibrous sheath of the flexor carpi radialis tendon	0
6	Tendon of the palmaris longus	0
7	Absence of APB	0

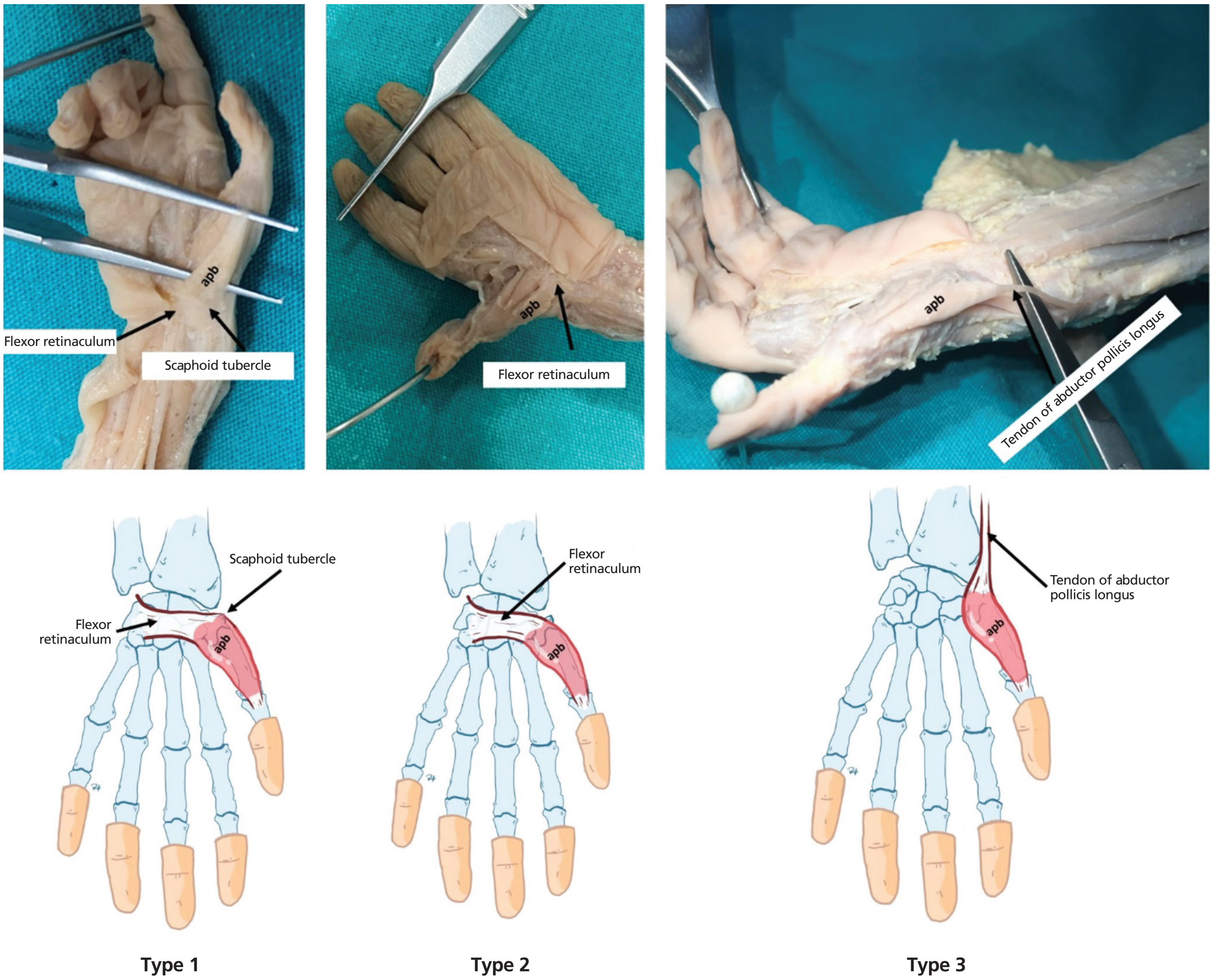

Figure 2. The types related to the origin of abductor pollicis brevis.

as the anteroposterior signaling center, governs growth from the index finger to the pinky finger. Disruptions in this axis can lead to digit anomalies, with polydactyly being an example of such a disruption. The third signaling hub, known as the dorsoventral center, directs growth from the upper side of the hand down to the palm. Interference with this signaling mechanism can result in the absence of certain fingers.[7] Anomalies in

Table 8
Description of types related to the insertion of APB in the literature.

Type	Descriptions of types (attachment sites)	n (%)
A	Lateral side of first metacarpophalangeal joint	40 (76.92)
B	Distal and lateral side of first metacarpal bone	9 (17.31)
C	Lateral side of first proximal phalanx	3 (5.77)
D	Absence of APB	0

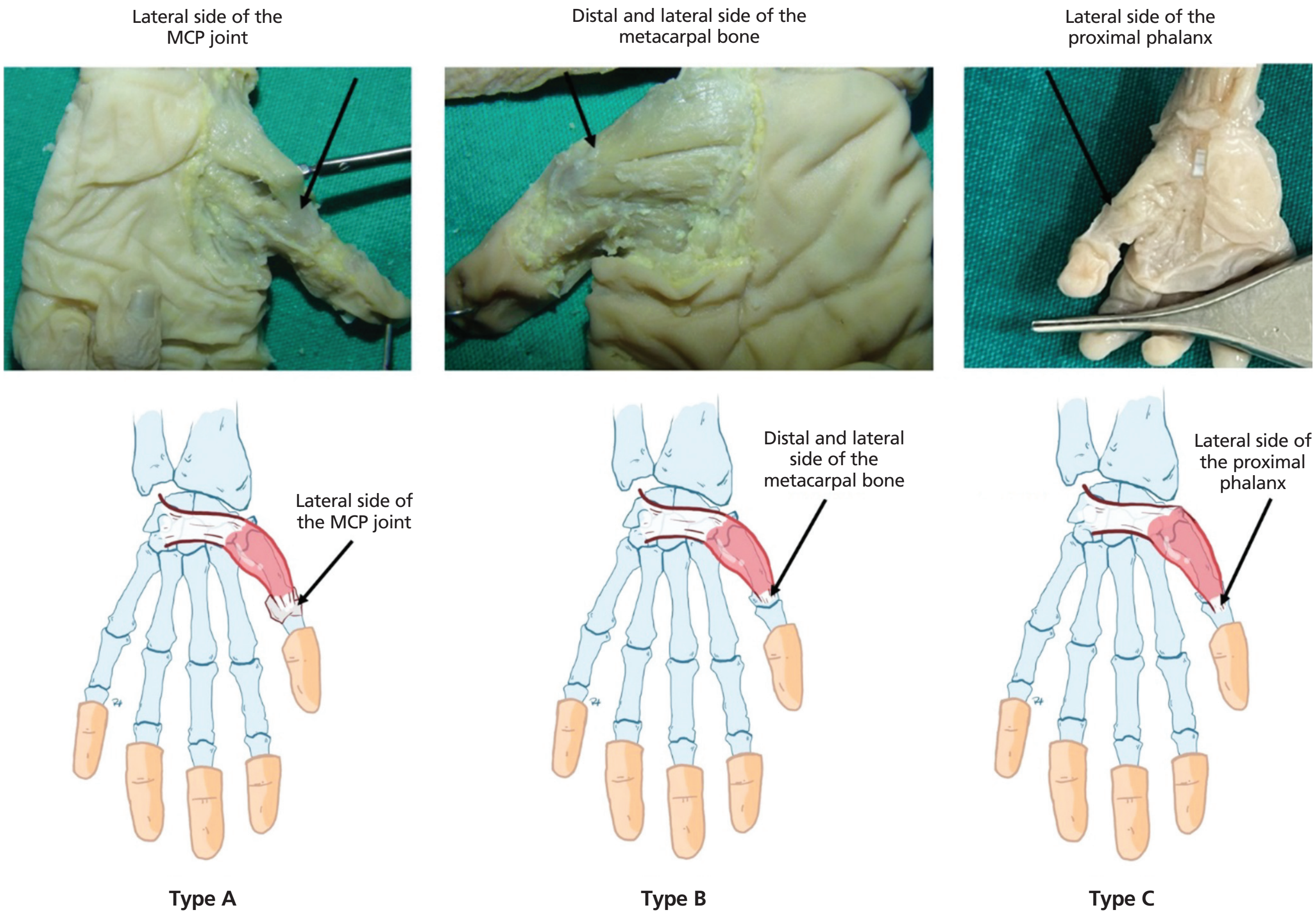

Figure 3. The types related to the insertion of abductor pollicis brevis.

the course of the APB have been reported in developmental thumb anomalies such as polydactyly and syndactyly.[3–4]

Several variations of the APB have been documented in the literature. These variations include absence of the muscle, double-headed muscle, triple-headed muscle with one head originating from the opponens pollicis, presence of the accessory slips (which may arise from the styloid process of the radius, scaphoid bone, abductor pollicis longus, extensor pollicis brevis, extensor pollicis longus, adductor pollicis, flexor pollicis brevis, opponens pollicis, accessory extensor carpi radialis, extensor carpi radialis longus, or palmaris longus) and fusion with the abductor pollicis longus.[2,11–14] In a 3D reconstruction study performed on an 8-week-old embryo, it was found that the opponens pollicis, flexor pollicis brevis and abductor pollicis brevis develop from a common muscle belly.[11] Additionally, in some cases, APB may insert to the radial sesamoid of the metacarpophalangeal joint and the dorsal extensor tendon hood.[15] This specific insertion of the APB is particularly significant in tendon transfer procedures, which are used to restore thumb opposition in cases of loss.[16]

Knowing the incidence of these variations in human fetuses is important for surgeries performed around thenar region, especially in newborns.[3,4,17] For instance, Carpenter et al.[17] successfully excised an extra finger in a 9-day-old newborn with polydactyly. Saito et al.[8] reported a strong correlation between the insertion level of APB and the bifurcation level of the radial thumb in individuals with polydactyly. Additionally, some authors have noted that variant attachments of the APB in subjects with polydactyly.[3,4]

To better understand its potential attachment points, we developed two classification systems encompassing different configurations related to the origin and insertion of

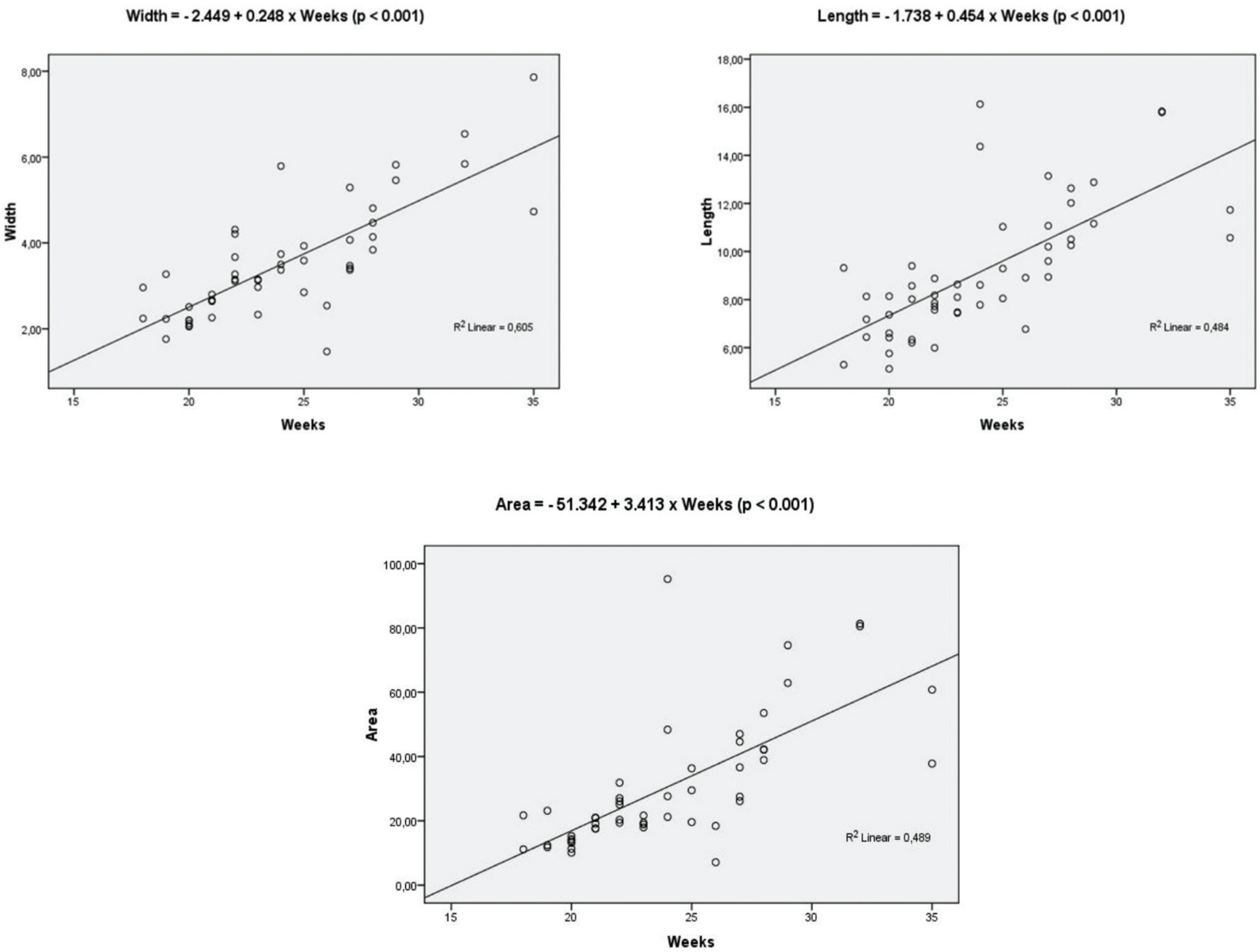

Figure 4. The linear function and scatter plots for the width, length and area of abductor pollicis brevis according to gestational weeks.

the muscle. Based on literature data, the origin and insertion of the APB were classified into seven and four types, respectively. These broad classification systems include all variations reported in previous studies. We then conducted a study on fetal subjects to determine the incidence of these types. In our findings, three different types related to the origin (Type 1 in 84.62% of sides, Type 2 in 11.54%, and Type 3 in 3.84%) and insertion (Type A in 76.92% of sides, Type B in 17.31%, and Type C in 5.77%) of the APB were observed. To the best of our knowledge, this study is the first to classify the origin and insertion of the APB in the literature. The classification we established for the origin of the APB may be particularly useful in surgical approaches, such as tendon transfer procedures for carpometacarpal joint osteoarthritis. In these procedures, which aim to stabilize the base of the first metacarpal bone, it is crucial to accurately determine the course and origin of the APB.[18,19] Our classification may provide valuable guidance in these types of surgeries.

In this study, the average APB area (APB-A), length (APB-L), and width (APB-W) were determined as 30.72 mm², 9.16 mm, and 3.53 mm, respectively. The morphometric characteristics of the muscle may be important for surgeons during procedures such as tendon transfer and muscle grafting.[5,18–21] For example, some authors have noted that underdeveloped thenar muscles can contribute to zigzag deformity of the thumb, and hypoplasia of the APB may lead to joint deformities.[20] In this study, the linear functions for APB-A, APB-L, and APB-W were calculated as follows: = -51.342+3.413

× weeks ($p<0.001$), $y = -1.738+0.454 \times$ weeks ($p<0.001$), and $y = -2.449+0.248 \times$ weeks ($p<0.001$), respectively. Considering the mean values and standard deviations from this study, these formulas may be particularly useful for estimating the size of the APB in fetuses.

This study does have some limitations. The number of fetal subjects was relatively small, so future studies with larger sample sizes could provide more comprehensive insights into the dimensions and variations of the APB, which may be beneficial for early childhood surgeries. Additionally, the anatomical features of the APB during the first trimester are important for understanding its embryonic development. In this study, the APB was observed to be distinguishable from the 15th week onward. However, the number of fetal samples in the first and third trimesters, particularly near term, was limited. Therefore, future studies should include anatomical examinations of fetal APB beyond 32 weeks to better inform early childhood surgeries. Further research in larger populations may provide more detailed information about the size and developmental patterns of the muscle.

Conclusion

The morphometric and morphological features of the APB are crucial for clinicians when performing surgical interventions around the thumb. To the best of our knowledge, this study is the first to classify the origin and insertion of the APB in human fetuses. Our classification systems may serve as a valuable guide for future studies, particularly those focused on thumb anomalies such as polydactyly and syndactyly in newborns, especially when conducted with larger sample sizes.

Conflict of Interest

The authors declare that they have no conflicts of interest.

Author Contributions

SSA: designed the research study, performed the research, analyzed the data and wrote the manuscript; SK: performed the research study; OB: designed the research study, contributed towards analytic tools, analyzed the data and wrote the manuscript; İB: designed the research study, performed the research, analyzed the data and wrote the manuscript; PK: manuscript writing and editing; MO: manuscript writing and editing. All authors have read and approve the final manuscript.

Ethics Approval

The study was conducted in accordance with the ethical rules of the Declaration of Helsinki and its later amendments.

Funding

None.

References

1. Warwick D, Logan J. Wrist and hand. In: Standring S, editor. Gray's anatomy: the anatomical basis of clinical practice. 42nd ed. Elsevier Limited; 2021. p. 955–90.
2. Gonzales MA, Netscher DT. Hand intrinsic muscles. In: Tubbs RS, Shoja MM, Loukas M, editors. Bergman's comprehensive encyclopedia of human anatomic variation. Hoboken (NJ): John Wiley & Sons, Inc.; 2016. p. 315–34.
3. Kozin SH, Zlotolow DA. Common pediatric congenital conditions of the hand. Plast Reconstr Surg 2015;136:241e–57e.
4. Tada K, Yonenobu K, Tsuyuguchi Y, Kawai H, Egawa T. Duplication of the thumb. A retrospective review of two hundred and thirty-seven cases. J Bone Joint Surg Am 1983;65:584–98.
5. Lourie GM, Costas BL, Bayne LG. The zig-zag deformity in preaxial polydactyly. A new cause and its treatment. J Hand Surg Br 1995;20:561–4.
6. Siqueira MA, Sterodimas A, Boriani F, Pitanguy I. A 10-year experience with the surgical treatment of radial polydactyly. Ann Ital Chir 2008;79:441–4.
7. Farrugia MC, Calleja-Agius J. Polydactyly: a review. Neonatal Netw 2016;35:135–42.
8. Saito S, Ueda M, Murata M, Suzuki S. Thenar dysplasia in radial polydactyly depends on the level of bifurcation. Plast Reconstr Surg 2018;141:85e–90e.
9. Malas M, Desticioğlu K, Cankara N, Evcil E, Özgüner G. Determination of fetal age during the fetal period. [Article in Turkish] Medical Journal of Süleyman Demirel University 2007; 14:20–4.
10. Warmbrunn MV, de Bakker BS, Hagoort J, Alefs-de Bakker PB, Oostra RJ. Hitherto unknown detailed muscle anatomy in an 8-week-old embryo. J Anat 2018; 233:243–54.
11. El-Beshbishy RA, Abdel-Hamid GA. Variations of the abductor pollicis longus tendon: an anatomic study. Folia Morphol (Warsz) 2013;72:161–6.
12. Fahrer M. On the form and function of the abductor pollicis brevis muscle. Aust N Z J Surg 1977;47:243–7.
13. Moore CW, Fanous J, Rice CL. Fiber type composition of contiguous palmaris longus and abductor pollicis brevis muscles: morphological evidence of a functional synergy. J Anat 2021;238:53–62.
14. Simard T, Roberge J. Human abductor pollicis brevis muscle "divisions" and the nerve hila. Anat Rec 1988;222:426–36.
15. Goldberg I, Nathan H. Anatomy and pathology of the sesamoid bones. Int Orthop 1987;11:141–7.
16. Roach SS, Short WH, Werner FW, Fortino MD. Biomechanical evaluation of thumb opposition transfer insertion sites. J Hand Surg Am 2001;26:354–61.
17. Carpenter CL, Cuellar TA, Friel MT. Office-based post-axial polydactyly excision in neonates, infants, and children. Plast Reconstr Surg 2016;137:564–8.

18. Heyworth BE, Jobin CM, Monica JT, Crow SA, Lee JH, Rosenwasser MP. Long-term follow-up of basal joint resection arthroplasty of the thumb with transfer of the abductor pollicis brevis origin to the flexor carpi radialis tendon. J Hand Surg Am 2009;34:1021–8.
19. Horch R, Stark GB. Abductor pollicis brevis muscle-plasty for therapy of radial collateral ligament rupture of the thumb base joint. Zentralbl Chir 1995;120:959–62.
20. Horch RE, Dragu A, Polykandriotis E, Kneser U. Radial collateral ligament repair of the thumb metacarpophalangeal joint using the abductor pollicis brevis tendon. Plast Reconstr Surg 2006;117:491–6.
21. Jacobson MD, Raab R, Fazeli BM, Abrams RA, Botte MJ, Lieber RL. Architectural design of the human intrinsic hand muscles. J Hand Surg Am 1992;17:804–9.

ORCID ID:
S. S. Adanır 0000-0002-9098-5194; S. Korkmaz 0000-0003-3423-8706; O. Beger 0000-0002-4932-8758; İ. Bahşi 0000-0001-8078-7074; P. Kervancıoğlu 0000-0003-3231-3637; M. Orhan 0000-0003-4403-5718

deomed®

Correspondence to: İlhan Bahşi, MD, PhD
Department of Anatomy, Faculty of Medicine,
Gaziantep University, Gaziantep, Türkiye
Phone: +90 342 360 60 60 / 4655
e-mail: dr.ilhanbahsi@gmail.com

Conflict of interest statement: No conflicts declared.

 How to cite this article: Adanır SS, Korkmaz S, Beger O, Bahşi İ, Kervancıoğlu P, Orhan M. Fetal anatomy of the abductor pollicis brevis and its clinical importance. Anatomy 2024;18(3):73–82.

Original Article

http://dergipark.org.tr/en/pub/anatomy
Received: September 22, 2024; Accepted: December 12, 2024
doi:10.2399/ana.24.1586683

anatomy
An International Journal of Experimental and Clinical Anatomy

Digit ratio: comparative analysis between professional volleyball players and medical students

Ozan Turamanlar[1], **İlknur Çöllü**[1], **Önder Çalışkan**[2]

[1]*Department of Anatomy, Faculty of Medicine, Izmir Kâtip Çelebi University, Izmir, Türkiye*
[2]*Department of Physiotherapy and Rehabilitation, Faculty of Health Sciences, Mudanya University, Bursa, Türkiye*

Abstract

Objectives: The ratio of the length of the 2nd digit to the 4th digit of the hand, known as the digit ratio (2D:4D), has been widely studied in health, behavioral, and sports sciences as a potential indicator of prenatal testosterone exposure. This study aimed to compare the 2D:4D ratios of male individuals who are athletically and academically successful and to evaluate whether 2D:4D can serve as a marker for occupational selection, talent identification, and the impact of individual characteristics on job performance.

Methods: This study included 32 male professional volleyball players and 39 male medical students. The lengths of the 2nd and 4th digits of both hands were measured using a digital caliper, and the 2D:4D ratio was calculated. The dominant hands of the participants were also recorded for analysis.

Results: Intra-group comparisons of the right-hand and left-hand 2D:4D ratios within both the student and volleyball player groups showed no statistically significant differences (p=0.225; p=0.922). Inter-group comparisons of the 2D:4D ratios for the right hand and left hand were also statistically similar (p=0.388; p=0.939). Additionally, the difference between the right-hand and left-hand 2D:4D ratios (Dr-l) did not differ significantly between the groups (p=0.525). Comparisons based on dominant hand preferences revealed no statistically significant findings.

Conclusion: This study highlights the need for larger, multicenter studies with more participants to further explore the potential relationship between 2D:4D ratios and occupational or performance traits. We hope this research serves as a foundation for future investigations and provides valuable insights for researchers in this field.

Keywords: digit ratio; medical students; performance; 2D:4D; volleyball players

Anatomy 2024;18(3):83–90

Introduction

One of the most frequently asked questions today is which profession young individuals are more likely to pursue or should pursue. Although various psychological and biological tests and methods have been utilized throughout history, providing a definitive answer to this question remains challenging. However, comparative, easily applicable, and low-cost tests may offer insights. Measurements related to an individual's physical structure, for instance, can provide clues about their personality traits, which could potentially simplify career selection. Digit ratios are one such commonly used measurement tool in physical assessments.[1]

The digit ratio, denoted as 2D:4D, refers to the ratio of the length of the 2nd digit (index finger = 2D) to the length of the 4th digit (ring finger = 4D).[2] These measurements are obtained by measuring from the midpoint of the basal creases on the ventral surface of the hand, where the digits meet the hand, to the tip of the digit (**Figure 1**).

There is evidence suggesting that the 2D:4D ratio negatively correlates with prenatal testosterone exposure

This study was an oral presentation at 24th National Anatomy Congress, 19th–21st September, 2024, Istanbul, Türkiye and positively correlates with estrogen levels.[3,4] Specifically, a low 2D:4D ratio is associated with higher prenatal testosterone and lower estrogen levels, while a high 2D:4D ratio correlates with lower testosterone and higher estrogen levels during fetal development.[4,5]

The 2D:4D ratio has been widely recognized as a potential marker of prenatal testosterone exposure across various fields, including health, behavioral sciences, and sports sciences. Research suggests that prenatal androgens influence brain development, enhancing its sensitivity to testosterone later in life. These hormones are thought to regulate brain structure and function, with 2D:4D often considered a reliable indicator of athletic potential.[6–8] A low 2D:4D ratio has been linked to success in financial endeavors, admission to medical schools, and strong performance in sports such as basketball, skiing, and football.[9–13] Elevated levels of fetal androgens are believed to contribute to the development of the cardiovascular system, improve visual-spatial skills, enhance physical stamina and speed, and increase tendencies toward aggressive behavior—traits that may provide competitive advantages in sports.[12,13]

The relationship between 2D:4D and academic performance has also been explored,[14–18] with some studies showing a negative correlation between 2D:4D and academic success.[14,16] However, there is limited research comparing individuals excelling in both physical and cognitive domains. Therefore, this study aims to compare the 2D:4D ratios of male individuals who are successful in sports with those who excel in academic fields. By doing so, we seek to investigate whether 2D:4D can serve as an indicator for career selection, talent identification, and assessing the impact of individual characteristics on job performance.

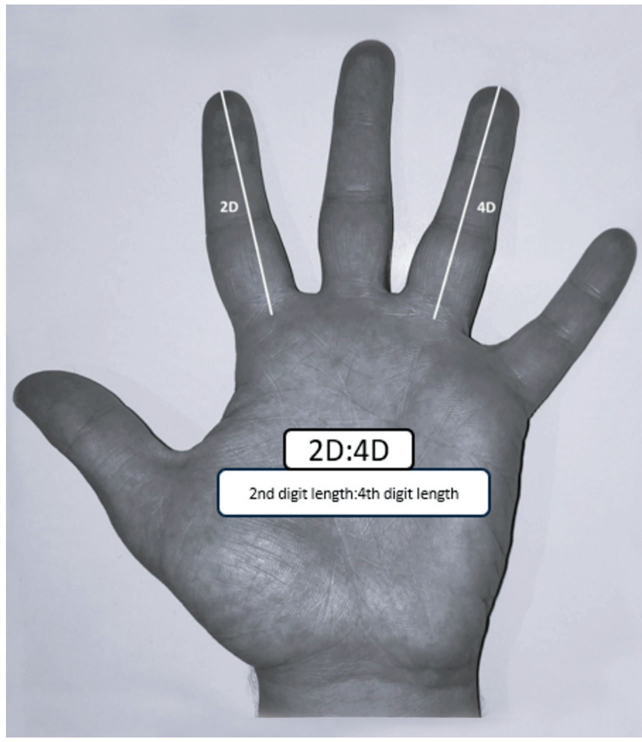

Figure 1. Measurement of digit lengths, left hand. **2D:** 2nd digit length; **4D:** 4th digit length.

Materials and Methods

Power analysis for two independent groups determined that the minimum required sample size was 68, with at least 32 participants in one group and 36 in the other. Under these conditions, the test power was estimated to be approximately 81.03%. In this study, we compared two groups: 32 male professional volleyball players competing in the top league (Efeler League) under the Turkish Volleyball Federation, and 39 male students from the Faculty of Medicine at Izmir Kâtip Çelebi University. The lengths of the 2nd and 4th digits of both hands were measured using a digital caliper (Rohs Norm 2002/95/EC) after obtaining informed consent from all participants. The 2D:4D ratio was calculated, and the dominant hands of the participants were recorded (**Figure 1**).

The exclusion criteria for this study included individuals with systemic diseases, finger anomalies or pathologies in any extremity, those under 18 years of age, and female participants to eliminate gender-related differences. Additionally, among the university student participants, individuals who engaged in any form of sports, even at an amateur level, were excluded.

Data analysis was conducted using IBM SPSS Statistics, version 26.0 (IBM Corp., Armonk, NY, USA). Summary statistics were presented as frequencies (n), percentages (%), mean ± standard deviation ($\overline{X}$± sd), median (M), minimum (min), and maximum (max) values. The Shapiro-Wilk test was used to assess the normality of numerical data, while the Levene test evaluated the homogeneity of variances. For comparisons between two groups, the “Independent two-sample t-test” was applied when parametric assumptions were met; otherwise, the “Mann-Whitney U test” was used. Intra-group and inter-group comparisons of right and left hand measurements

Table 1
Participant characteristics.

Participant	Right-handed n (%)	Left-handedn (%)	Total (n)
Volleyball players	29 (90.62%)	3 (9.38%)	32
University students	35 (89.74%)	4 (10.26%)	39
Total	64 (90.14%)	7 (9.86%)	71

n: number of participants.

were analyzed using "Mixed Order ANOVA." Statistical significance was defined as $p<0.05$.

Results

The number of participants and their hand dominance are presented in **Table 1**. The 32 volleyball players had an average age of 26.96 years, an average height of 193.40 cm, and an average weight of 83.75 kg (**Table 2**). The 39 university students had an average age of 20.74 years, an average height of 178.64 cm, and an average weight of 75.16 kg (**Table 3**).

Intra-group comparisons of the right-hand and left-hand 2D:4D ratios within the student and volleyball player groups showed no statistically significant differences (**Table 4**). Similarly, inter-group comparisons of the right-hand and left-hand 2D:4D ratios were statistically similar (**Table 4**). The inter-group comparison of the difference between the right-hand and left-hand 2D:4D ratios (Dr-l) also showed no significant differences (**Table 5**).

When participants were grouped by hand dominance, the right-hand 2D:4D, left-hand 2D:4D, and Dr-l values were statistically similar for both right-handed (**Table 6**) and left-handed dominant participants (**Table 7**). Of the total participants, 64 were right-handed dominant and 7 were left-handed dominant. Analysis of right-hand 2D:4D, left-hand 2D:4D, and Dr-l values, grouped by dominant hand, did not yield any statistically significant results (**Table 8**).

Table 2
Demographic characteristics of volleyball players.

Variables	n	Min-Max	Mean±SD
Age (years)	32	18–49	26.96±8.33
Height (cm)	32	180–210	193.40±7.19
Weight (kg)	32	68–112	83.75±9.68

Max: maximum; **Min:** minimum; **n:** number of participants; **SD:** standard deviation.

Table 3
Demographic characteristics of university students..

Variables	n	Min-Max	Mean±SD
Age (years)	39	19–26	20.74±1.48
Height (cm)	39	160–191	178.64±7.47
Weight (kg)	39	54–111	75.16±12.91

Max: maximum; **Min:** minimum; **n:** number of participants; **SD:** standard deviation.

Table 4
Comparison of 2D:4D values within and between groups.

		Groups		Test statistics*		
		Student	Player	F	p-value	η^2
2D:4D value	Right	0.9863±0.0408	0.9932±0.0212	0.754	0.388	0.011
	Left	0.9921±0.0429	0.9927±0.0247	0.006	0.939	0.001
Test statistics†		F=1.498 p=0.225 η^2=0.021	F=0.010 p=0.922 η^2=0.001			

F: mixed design ANOVA; η^2: effect size; *comparison between groups: †comparison within groups. Descriptive statistics are given as mean±standard deviation. The statistical significance level is $p<0.05$.

Table 5
Comparison of Dr-l (right hand) in groups (2D:4D minus left hand 2D:4D difference).

		Groups		Test statistics	
		Student	**Player**	**z-value**	**p-value**
Dr-l	$\bar{x}$±sd	-0.0058±0.0338	0.0005±0.0229	0.636	0.525
	M (min-max)	-0.0021 (-0.10–0.07)	-0.0002 (-0.06–0.06)		

$\bar{x}$: mean; **sd:** standard deviation; **M:** median; **z:** Mann-Whitney U test.

Table 6
Comparison by group in right dominant hands (Dr-l:Right hand 2D:4D minus left hand 2D:4D difference).

		Groups		Test statistics	
		Student	**Player**	**Test value**	**p-value**
2D:4D right	$\bar{x}$±sd	0.9874±0.0412	0.9938±0.0226	z=0.636	0.525
	M (min-max)	0.9939 (0.9008–1.1092)	0.9942 (0.9509–1.0356		
2D:4D left	$\bar{x}$±sd	0.9921±0.0433	0.9927±0.0264	z=0.298	0.766
	M (min-max)	0.9854 (0.9031–1.1041)	0.9893 (0.9550–1.0669)		
Dr-l	$\bar{x}$±sd	-0.0047±0.0350	0.0011±0.0243	t=0.753	0.454
	M (min-max)	0 (-0.10–0.07)	0.0006 (-0.06–0.06)		

$\bar{x}$: mean; **sd:** standard deviation; **M:** median; **t:** independent two-sample t test; **z:** Mann-Whitney U test.

Table 7
Comparison by group in left dominant hands (Dr-l: Right hand 2D:4D minus left hand 2D:4D difference).

		Groups		Test statistics	
		Student	**Player**	**t-value**	**p-value**
2D:4D right	$\bar{x}$±sd	0.9733±0.0416	0.9893±0.0072	0.775	0.474
	M (min-max)	0.9850 (0.9270–1.0079)	0.9910 (0.9769–0.9955)		
2D:4D left	$\bar{x}$±sd	0.9915±0.0475	0.9930±0.0047	0.063	0.952
	M (min-max)	1.0131 (0.9370–1.0244)	0.9918 (0.9891–0.9991)		
Dr-l	$\bar{x}$±sd	-0.0182±0.0091	-0.0037±0.0081	0.221	0.078
	M (min-max)	-0.016 (-0.03–0.01)	-0.025 (-0.01–0.0)		

$\bar{x}$: mean; **sd:** standard deviation; **M:** median; **t:** independent two-sample t test.

Table 8
Comparison according to the dominant hand (Dr-l: Right hand 2D:4D minus left hand 2D:4D difference).

		Groups		Test statistics	
		Right handed dominant	**Left handed dominant**	**z-value**	**p-value**
2D:4D right	$\bar{x}$±sd	0.9902±0.0342	0.9824±0.0260	0.775	0.474
	M (min-max)	0.9940 (0.9008–1.1092)	0.9877 (0.9270–1.0079)		
2D:4D left	$\bar{x}$±sd	0.9924±0.0366	0.9923±0.0276	0.501	0.616
	M (min-max)	0.9877 (0.9031–1.1041)	0.9944 (0.9370–1.0244)		
Dr-l	$\bar{x}$±sd	-0.0022±0.0307	-0.0099±0.0110	0.215	0.210
	M (min-max)	0.0006 (-0.10–0.07)	-0.0100 (-0.03–0.0)		

$\bar{x}$: mean; **sd:** standard deviation; **M:** median; **z:** Mann-Whitney U test.

Discussion

Prenatal testosterone levels may play a pivotal role in excelling at certain sports activities. Traits influenced by testosterone, such as muscle fiber growth, enhanced strength, reduced fat mass, and elevated hematocrit levels, are likely contributors to athletic success.[19] The 2D:4D ratio has been shown to correlate with performance in various individual and team sports, including basketball, skiing, volleyball, fencing, and football.[12,13,20–22]

In a study comparing athletes in judo, wrestling, and kickboxing with a control group of non-athletes, the 2D:4D ratio was found to be significantly lower in the athlete group.[23] This finding aligns with research suggesting that a low 2D:4D ratio is associated with elevated testosterone levels and tendencies toward aggression, traits often beneficial in combat sports.[24–26] Additionally, athletes participating in contact sports have been reported to have significantly lower 2D:4D ratios compared to those in non-contact sports.[7] Reed and Meggs[7] found that athletes in contact sports exhibited both lower 2D:4D ratios and higher physical aggression compared to their non-contact counterparts.

The population of study included the male athletes belonged to a professional volleyball team, representing a non-contact sport. The lack of a statistically significant difference in the 2D:4D ratio among professional athletes in our study may be attributed to their involvement in a non-contact sport.

Manning et al.[26] found that the right-hand 2D:4D ratio is more sensitive to prenatal sex steroids than the left-hand 2D:4D. Similarly, Hönekopp and Watson,[25] in their 2010 meta-analysis, reported higher prenatal androgenization in the right-hand 2D:4D compared to the left-hand 2D:4D. Research on 2D:4D generally examines both right- and left-hand ratios, while also considering the difference between them (Dr-l) as an additional marker. This difference, calculated as the right-hand 2D:4D minus the left-hand 2D:4D, has been proposed as a negative marker for prenatal testosterone exposure and a positive marker for prenatal estrogen exposure.[26] Dr-l is sexually dimorphic, with males consistently exhibiting lower values than females. This distinction emphasizes its potential as a marker for prenatal hormone exposure. Hill et al. identified a negative correlation between lower Dr-l values and VO2 max.[27] VO2 max, the maximum rate of oxygen consumption during exercise, reflects cardiovascular capacity and determines the upper limit of performance in endurance sports.[28] The regulatory effects of prenatal testosterone on the developing cardiovascular system may influence aerobic performance levels later in life.

Kim et al.[29] also reported that the right hand tends to exhibit stronger sex differences and is more sensitive to prenatal androgens compared to the left hand. For instance, in a study conducted on female Olympic athletes, only the right-hand 2D:4D showed a significant difference compared to the control group, while in another study on gymnast girls, the left-hand 2D:4D did not show a significant difference from the control group.[30,31] Although the digit ratio of the right and left hands was not found to be associated with hand preference, the Dr-l (difference between right-hand and left-hand 2D:4D) was shown to be linked to hand preference. Studies have found that left-handed individuals exhibit significantly lower Dr-l values compared to right-handed individuals.[32,33] This suggests that considering hand dominance in future research may help in interpreting the results more accurately. The results of our study showed no significant relationship between Dr-l and hand dominance in the statistical analyses. However, this result may be attributed to the relatively small sample size, which could have limited the statistical power to detect significant differences. It is suggested that future studies with larger sample sizes be conducted to clarify this relationship.

It is recognized that 2D:4D ratios vary among individuals from different ethnic groups, regardless of sport. In a study, average 2D:4D values were reported to differ between ethnic groups, irrespective of gender.[34] Therefore, ethnic differences should be considered in future research, as the current study was conducted on a Turkish population. In a study conducted in India, volleyball players were compared with a control group, and the 2D:4D ratios of both hands were found to be significantly lower in volleyball players. However, no statistically significant difference in Dr-l was observed between the volleyball players and the controls.[21] In the present study, male university students with no prior involvement in sports were compared with professional male volleyball players, but no significant differences were detected in the statistical analysis.

In a study examining the association between 2D:4D and performance in both practical and theoretical exams among dental students in Brazil, a significant negative correlation was found between 2D:4D and exam scores in male students.[16] Similarly, Coco et al.[14] reported a notable relationship between 2D:4D and success in medical school entrance exams in Italy. Additionally, a multicenter study conducted across Russia and the Philippines identified a non-linear, quadratic correlation between 2D:4D and academic success.[17]

It has been proposed that prenatal testosterone influences cognitive abilities, such as intelligence and learning, by affecting key developmental processes, including neuronal proliferation, migration, differentiation, and apoptosis. This influence is thought to enhance the density of neural networks in specific brain regions.[35] Prenatal exposure to testosterone may directly affect intelligence by altering neuronal migration, leading to greater development of the right hemisphere and improved coordination within and between hemispheres.[36] This process promotes the development and organization of dense neuronal networks in areas associated with cognition, learning, and memory, potentially through reduced apoptosis or increased neuronal migration to these regions during development.[6,35] Androgens have also been shown to have an organizational effect on brain development, suggesting that prenatal testosterone may act as a programming mechanism that influences behavior later in life.[37] Supporting this, a study found that individuals presenting with "boxer's fracture" had significantly lower 2D:4D ratios compared to the general population, linking 2D:4D to physical and behavioral traits associated with testosterone exposure.[38]

It has been reported in several studies that no significant correlation exists between 2D:4D and physical performance. It has also been suggested that claims regarding a relationship may be somewhat overstated. Based on these findings, it is indicated that 2D:4D is unlikely to serve as a reliable predictive marker for athletes' physical performance and abilities.[39–41] In the present study, the absence of statistically significant differences in the results may be attributed to the limited sample size and the lack of additional measurement parameters.

Conclusion

Studies have shown that digit ratios can reflect performance across various domains. In our study, comparisons were made between volleyball players who had achieved a high level of physical performance and medical students who demonstrated their abilities through academic success. No significant differences were found between the measurement results of the two groups. It is suggested that the lack of differences observed in our study may stem from the fact that both groups excelled in their respective fields. This indicates that 2D:4D may be more closely associated with behavioral characteristics rather than being limited to specific activities or professions.

Future studies should consider larger sample sizes and include a broader range of populations. It would also be valuable to examine the relationship between digit ratios and specific psychological or personality traits using validated tests. However, it is essential to approach such associations cautiously, taking into account the potential influence of cultural differences on the validity and reliability of these tests.

We believe that our study can serve as a foundation for more detailed analyses to be conducted in multicenter studies with larger participant groups. It also provides a valuable perspective for researchers interested in exploring this area further.

Conflict of Interest

All authors participating in the study declare that there is no conflict of interest regarding the study.

Author Contributions

OT: project development, data management, data analysis, manuscript writing, manuscript editing; İÇ: project development, data collection, data analysis, manuscript writing, manuscript editing; ÖÇ: data collection.

Ethics Approval

Necessary permissions for this study were obtained from the Izmir Kâtip Çelebi University Clinical Research Ethics Committee (approval number: 2022/587). The study was conducted in accordance with the principles outlined in the Declaration of Helsinki on Human Rights.

Funding

None.

References

1. Serpell BG, Cook CJ. Exploring finger digit ratios (2D:4D) in surgeons, professional rugby players, and political journalists to form a directional hypothesis: could finger length predict attention and focus? Front Behav Neurosci 2022;16:873129.
2. Manning JT, Scutt D, Wilson J, Lewis-Jones DI. The ratio of 2nd to 4th digit length: a predictor of sperm numbers and concentrations of testosterone, luteinizing hormone and oestrogen. Hum Reprod 1998;13:3000–4.
3. Manning JT. Digit ratio: a pointer to fertility, behavior, and health. New Brunswick (NJ): Rutgers University Press; 2002. p. 198.

4. Robinson S. The ratio of 2nd to 4th digit length and male homosexuality. Evol Hum Behav 2000;21:333–45.
5. Crewther B, Cook C, Kilduff L, Manning J. Digit ratio (2D:4D) and salivary testosterone, oestradiol and cortisol levels under challenge: evidence for prenatal effects on adult endocrine responses. Early Hum Dev 2015;91:451–6.
6. Lenz B, Müller CP, Stoessel C, Sperling W, Biermann T, Hillemacher T, Bleich S, Kornhuber J. Sex hormone activity in alcohol addiction: integrating organizational and activational effects. Prog Neurobiol 2012;96:136–63.
7. Reed S, Meggs J. Examining the effect of prenatal testosterone and aggression on sporting choice and sporting longevity. Personality and Individual Differences 2017;116:11–5.
8. Alonso J, Di Paolo R, Ponti G, Sartarelli M. Facts and misconceptions about 2D:4D, social and risk preferences. Front Behav Neurosci 2018;12:22.
9. Coates JM, Gurnell M, Rustichini A. Second-to-fourth digit ratio predicts success among high-frequency financial traders. Proc Natl Acad Sci U S A. 2009;106:623–8.
10. Coco M, Perciavalle V, Maci T, Nicoletti F, Di Corrado D, Perciavalle V. The second-to-fourth digit ratio correlates with the rate of academic performance in medical school students. Mol Med Rep 2011;4:471–6.
11. Keith-Barnett N, Campbell A. Sporting achievement: what is the contribution of digit ratio? Journal of Personality 2007;75:663–78.
12. Manning JT. The ratio of 2nd to 4th digit length and performance in skiing. J Sports Med Phys Fitness 2002;42:446–50.
13. Manning JT, Taylor RP. Second to fourth digit ratio and male ability in sport: implications for sexual selection in humans. Evol Hum Behav 2001;22:61–9.
14. Coco M, Perciavalle V, Maci T, Nicoletti F, Di Corrado D, Perciavalle V. The second-to-fourth digit ratio correlates with the rate of academic performance in medical school students. Mol Med Rep 2011;4:471–6.
15. Tektas OY, Kapsner L, Lemmer M, Bouna-Pyrrou P, Lewczuk P, Lenz B, Kornhuber J. Digit ratio (2D:4D) and academic success as measured by achievement in the academic degree “Habilitation”. PLoS One 2019;14:e0212167.
16. Hopp RN, De Moraes JP, Jorge J. Digit ratio and academic performance in dentistry students. Personality and Individual Differences 2012;52:643–6.
17. Nye JVC, Androuschak G, Desierto D, Jones G, Yudkevich M. 2D:4D asymmetry and gender differences in academic performance. PLoS One 2012;7:e46319.
18. Anas YI, Badamasi MI. Relationship between second to fourth digit ratio (2D:4D) and academic performance among students in Nigeria. Bayero Journal of Pure and Applied Sciences 2021;13:87–93.
19. Moffit DM, Swanik CB. The association between athleticism, prenatal testosterone, and finger length. J Strength Cond Res 2011;25:1085–8.
20. Frick NA, Hull MJ, Manning JT, Tomkinson GR. Relationships between digit ratio (2D:4D) and basketball performance in Australian men. Am J Hum Biol 2017;29:e22937.
21. Panda K, Majumdar P, Umesh V, Sudhakar H. Ratio of second to fourth digit as a predictor of performance in elite Indian volley ball players. National Journal of Physiology, Pharmacy and Pharmacology 2014;4:106–8.
22. Voracek M, Reimer B, Dressler SG. Digit ratio (2D:4D) predicts sporting success among female fencers independent from physical, experience, and personality factors. Scand J Med Sci Sports 2010; 20:853–60.
23. Adamczyk JG, Safranow K, Gajewski AK, Boguszewski D, Sozański H, Sołtyszewski I, Pepłońska B, Cięszczyk P, Siewierski M, Żekanowski C. The second–to–fourth digit (2D:4D) ratio of male combat athletes is associated with the choice of sport. J Hum Kinet 2021;78:59–66.
24. Ribeiro E, Neave N, Morais RN, Kilduff L, Taylor SR, Butovskaya M, Fink B, Manning JT. Digit ratio (2D:4D), testosterone, cortisol, aggression, personality and hand-grip strength: evidence for prenatal effects on strength. Early Hum Dev 2016; 100:21–5.
25. Hönekopp J, Watson S. Meta–analysis of digit ratio 2D:4D shows greater sex difference in the right hand. Am J Hum Biol 2010;22: 619–30.
26. Manning J, Kilduff L, Cook C, Crewther B, Fink B. Digit ratio (2D:4D): a biomarker for prenatal sex steroids and adult sex steroids in challenge situations. Front Endocrinol (Lausanne) 2014; 5:9.
27. Hill R, Simpson B, Manning J, Kilduff L. Right–left digit ratio (2D:4D) and maximal oxygen uptake. J Sports Sci 2012;30:129–34.
28. Lombardo MP, Otieno S. The associations between digit ratio, aerobic fitness, physical skills, and overall physical fitness of elite youth distance runners. Am J Hum Biol 2021;33:e23448.
29. Kim Y, Kim K, Kim TH. Domain specific relationships of 2D:4D digit ratio in risk perception and risk behavior. J Gen Psychol 2014; 141:373–92.
30. Eklund E, Ekström L, Thörngren JO, Ericsson M, Berglund B, Hirschberg AL. Digit ratio (2D:4D) and physical performance in female olympic athletes. Front Endocrinol (Lausanne) 2020;11: 292.
31. Peeters MW, Claessens AL. The left hand second to fourth digit ratio (2D:4D) does not discriminate world-class female gymnasts from age matched sedentary girls. PLoS One 2012;7:e40270.
32. Beaton AA, Rudling N, Kissling C, Taurines R, Thome J. Digit ratio (2D:4D), salivary testosterone, and handedness. Laterality 2011;16:136–55.
33. Stoyanov Z, Marinov M, Pashalieva I. Finger length ratio (2D:4D) in left- and right-handed males. Int J Neurosci 2009;119:1006–13.
34. Manning JT, Churchill AJG, Peters M. The effects of sex, ethnicity, and sexual orientation on self-measured digit ratio (2D:4D). Arch Sex Behav 2007;36:223–33.
35. Mrazik M, Dombrowski SC. The neurobiological foundations of giftedness. Roeper Review 2010;32:224–34.
36. Alexander JE, O’Boyle MW, Benbow CP. Developmentally advanced EEG alpha power in gifted male and female adolescents. Int J Psychophysiol 1996;23:25–31.
37. Lombardo MV, Ashwin E, Auyeung B, Chakrabarti B, Lai MC, Taylor K, Hackett G, Bullmore ET, Baron-Cohen S. Fetal programming effects of testosterone on the reward system and behavioral approach tendencies in humans. Biol Psychiatry 2012;72:839–47.

38. Joyce CW, Kelly JC, Chan JC, Colgan G, O'Briain D, Mc Cabe JP, Curtin W. Second to fourth digit ratio confirms aggressive tendencies in patients with boxers fractures. Injury 2013;44:1636–9.

39. Özden Yurdakul H, Özen G, Koç H. The relationship between digit ratio (2D:4D), anaerobic power and athletic ability of young athletes. Universal Journal of Educational Research 2018;6:2913–7.

40. Çel A, Aksu F, Tunar M, Da EN, Ada D, Topaço H. The relationship between physical performance levels and the digit ratio of master athletes. [Article in Turkish] Dokuz Eylül Üniversitesi Tıp Fakültesi Dergisi 2020;1:5–10.

41. Peeters MW, Claessens AL. Digit ratio (2D:4D) and competition level in world-class female gymnasts. J Sports Sci 2013;31:1302–11.

ORCID ID:
O. Turamanlar 0000-0002-0785-483X;
İ. Çöllü: 0000-0003-1605-6327;
Ö. Çalışkan: 0009-0000-5537-258X

deomed®

Correspondence to: İlknur Çöllü, MD
Department of Anatomy, Faculty of Medicine,
Izmir Kâtip Çelebi University, Izmir, Türkiye
Phone: +90 507 258 02 10
e-mail: ilknurcollu1@gmail.com

Conflict of interest statement: No conflicts declared.

Original Article

http://dergipark.org.tr/en/pub/anatomy
Received: June 5, 2024; Accepted: November 28, 2024
doi:10.2399/ana.24.1496367

anatomy
An International Journal of Experimental and Clinical Anatomy

Undernutrition in the last period of lactation may have adverse effects on skeletal development

Hakan Ay, Ferruh Yücel

Department of Anatomy, Faculty of Medicine, Eskişehir Osmangazi University, Eskişehir, Türkiye

Abstract

Objectives: Malnutrition in childhood causes permanent damage. Studies report that there are different developmental mechanisms at different stages of breastfeeding. Our study aims to observe the effects of undernutrition in the first and last weeks of lactation on body weight and skeletal development after rehabilitation until puberty, and ultimately to reveal which period of lactation is more critical.

Methods: Lactating rats were undernourished by receiving half the diet consumed by control mothers during the first (0–7th day, U1 group) or third (14–21st day, U2 group) week of lactation. Rats were weighed each week and radiographs were taken on the 21st and 49th days. All measurements were taken directly on the radiographs.

Results: On day 49, the body weight and body length of the two undernourished groups were lower than those of the controls. U2 was behind in all measurements except head, pelvic, iliac, and ischial lengths. U2 also lagged behind U1 in body, tail, spine, upper limb, and tibia lengths. While U1 did not differ from controls in many measurements, femur length, bi-iliac, bi-acetabular, and ischial width were less than controls.

Conclusion: Undernutrition in the last week of lactation affected body weight and skeletal development more than malnutrition in the first postnatal week.

Keywords: lactation; radiograph; rat; skeletal development; undernutrition

Anatomy 2024;18(3):91–100

Introduction

The growing world population brings with it the problem of malnutrition. The global nutrition crisis we faced even before Covid-19[1] has become far worse, with worrying trends across every form of malnutrition, from hunger to obesity. People affected by hunger leaped by 150 million since the Covid-19 outbreak, from 618 million in 2019 to 768 million in 2021, while those unable to afford a healthy diet[2] rose by 112 million to 3.1 billion in 2020 alone.[3] Almost a third (29.3%) of the world's population, 2.3 billion people, were moderately or severely food insecure[4] in 2021, up from 25.4% before the pandemic.[5] At the same time, what we eat across the world continues to fall short of the minimum standards for healthy and sustainable diets[6] with resulting obesity and diet-related non-communicable diseases (NCDs) on the rise and at epidemic levels – around 40% of all adults and 20% of all children are now overweight or obese.[7] Policy interventions to date are failing to reverse these trends, while conflict around the world and the impacts of climate change, which are key drivers of increases in malnutrition, continue unabated.[8]

Many studies have investigated the effects of malnutrition on body weight of rats at different ages. Most of these studies found that undernutrition of rats before weaning can lead to permanent defects in body weight.[9–12] However, body weight alone is not a sufficient parameter to indicate growth; additional indicators are needed, such as body length and skeletal growth. Using skeletal growth to monitor the effects of nutritional intervention provides a more reliable method of measuring growth retardation.[13] Several studies have examined the effects of malnutrition on skeletal development. Some of these studies examined the effects of undernutrition on skeletal development after weaning and others before weaning. However, some studies include both periods.[14–16] Studies have shown that growth and development occur through different mechanisms at different stages of lactation.[17,18]

Previous studies do not provide detailed comparative information on the effects of undernutrition during the first and last weeks of lactation on skeletal development and body weight in rats. In this study, we aimed to observe skeletal development and body weight of rats exposed to undernutrition during the first and last week of lactation and rehabilitation until puberty, and finally to find out which period of lactation is more critical for skeletal development.

Materials and Methods

Eight female Wistar albino rats weighing approximately 210 g were used for this study. The animals were kept under standard conditions (21°C, 12h light/dark cycle) and had ad libitum access to food and water. After overnight mating with male rats, females were classified as pregnant with sperm in the vaginal smear. Pregnant females gave birth to pups approximately 21 days after mating. Pups born on the same day were divided according to sex, and male pups were distributed in groups of 8 to three different mothers. Birth weights (P0) were weighed using a precision balance (310M, Precisa, Dietikon, Switzerland). This procedure was repeated every week until day 49 (P49).

The experimental groups were undernourished at different time points during the 21-day breastfeeding period. The first group (U1) was undernourished between P0 and P7, and the second group was undernourished between P14 and P21. The undernutrition protocol was implemented by giving the experimental groups half of the food that the control group (C) ate on the same days (Oğuzlar Tarim Urunleri Sanayi ve Ticaret A.S. Eskisehir-Türkiye, for the content of the food, see **Table 1**). According to this, the U1 mother was undernourished with 10 g of food at P0 to P3 and 15 g at P4 to P7. In contrast, the U2 mother received 20 g of feed at P14 and 25 g at P15 to P21. On the other days of lactation, the mothers had access to food ad libitum.

At the end of day 21, all pups were separated from their mothers and anesthetized with an intramuscular injection of 50 mg/kg ketamine (Ketalar, Zentiva, Luleburgaz, Türkiye). Rats were placed ventrally on an X-ray cassette according to the study by Hughes and Tanner (1970) (**Figure 1**).[19] Radiographs were taken with a Philips Diagnostic PCS 2000 X-Ray machine

Table 1
Composition of the rat chow.

Essential Nutrients Included (%)	
Dry matter	88 min.
Protein	16 min.
Cellulose	14 min.
Ash	9 max.
Calcium	0.8-1.5 min.-max.
Phosphorus	0.5 min.
Sodium	0.2-0.4 min.-max.
NaCl	1.00 max.
Energy (Kcal/kg)	2400 min.
Vitamins (IU/kg)	
Vitamin A	5000 min.
Vitamin D3	1000 min.
Vitamin E	30 min.

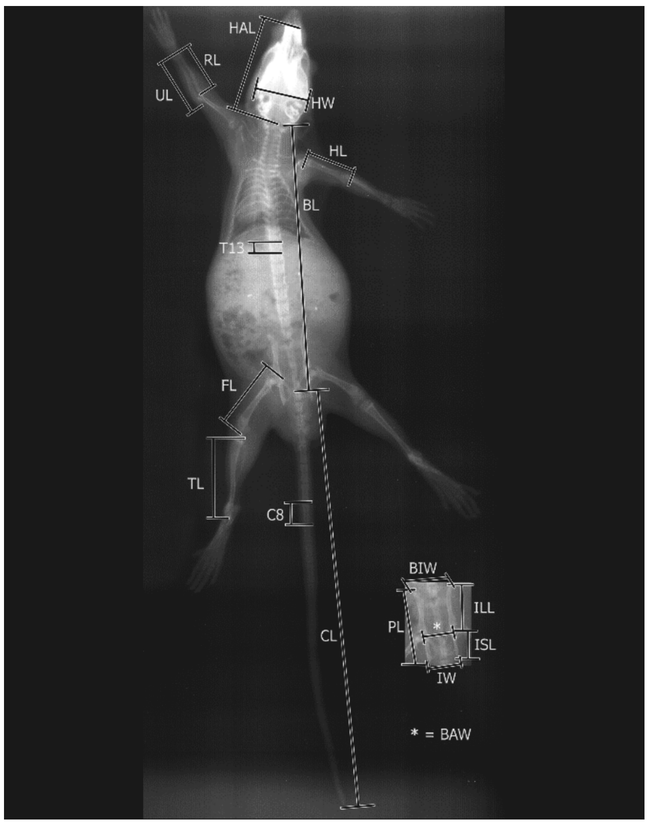

Figure 1. Measurements made on radiographs. The radiograph was taken on 21st day (P21). **BAW:** bi-acetabular width; **BIW:** bi-iliac width; **BL:** body length; **C8:** length of the 8th caudal vertebra; **CL:** tail length; **FL:** length of the left femur; **HW:** head width; **HAL:** head length; **HL:** length of the right humerus; **ILL:** iliac length; **ISL:** ischial length; **IW:** ischial width; **PL:** pelvic length; **RL:** (length of the left Radius), **T13:** length of the 13th thoracic vertebra; **TL:** length of the left tibia; **UL:** length of the left ulna.

from a distance of 120 cm with a dose of 41 kV-2 mA. On day 49, second radiographs were taken in the same manner.

All measurements were made by the same observer directly on radiographs using a caliper with an accuracy of 0.05 mm (Izeltas, Izmir, Türkiye). Body and tail length were measured with a thread shaped according to the shape of the structures. All measurements were taken three times and the average of these measurements was taken into account. The dimensions of the skeleton were measured in previous studies and certain relevant landmarks were considered in all measurements.[13,19–23]

Data sets were analyzed for normality using the Kolmogorov-Smirnov test and compared with ANOVA (Tukey posthoc tests) using JAMOVI 2.3.28 software.

Results

Body weights

There was no significant difference between the birth weights of the groups at P0. At P7, it was observed that the body weight of U1 was lower than that of the normally fed groups. Although all groups were fed normally between P7 and P14, the body weight of nutritionally damaged U1 remained lower than that of the other groups. At P21, the body weight of undernourished U2 was lower than that of the other two groups; meanwhile, the body weight of U1 had risen above that of C. At P28, the body weight of U2 was still lower than that of the other two groups. At P35, C's body weight was higher than that of the experimental groups, while U2's body weight was also lower than that of U1 on that day. At P42, the body weight of the experimental groups remained lower than that of C, but the body weight of U1 remained higher than that of U2. The final weights measured at P49 showed that the body weights of the experimental groups were still lower than that of C, but the difference between the experimental groups disappeared (**Figure 2**).

In terms of growth rates, it can be seen that the growth rate of U1 between P0–7 was 78% of C and the growth rate of U2 was 98%. The growth rates of the

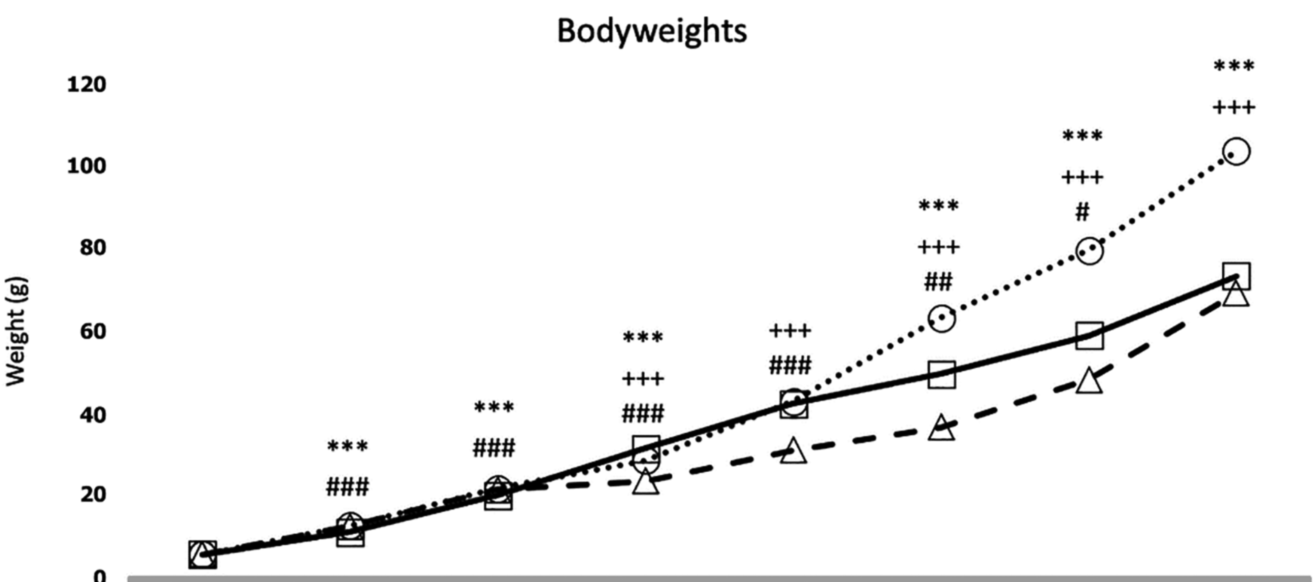

	P0	P7	P14	P21	P28	P35	P42	P49
C	5.5±0.6	12.5±0.5	21.6±0.4	28.5±0.4	42.9±6.5	63.2±9.6	79.6±12.3	103.8±14.8
U1	5.5±0.5	11.0±0.4	19.9±0.5	31.4±0.9	42.3±2.3	49.5±3.6	58.9±5.5	73.4±1.3
U2	5.5±0.7	12.4±0.5	21.3±0.4	23.4±0.6	30.9±1.8	36.6±3.6	48.2±5.5	69.2±3.4

Days

Figure 2. Body weights weighed from day 0 (P0) to day 49 (P49) (±standard deviation), n=8. **C:** control group; **U1:** the first group that was undernourished between day 0 (P0) and day 7 (P7); **U2:** the second group that was undernourished between day 14 (P14) and day 21 (P21); sig: significancy; *: comparison of C with U1; +: comparison of C with U2; #: comparison of U1 with U2. One symbol means p<0.05; two means p<0.01; three means p<0.001.

groups between P7–14 were similar (98%). Between P14–21, the growth rate of malnourished U2 was very low (31%), while the growth rate of U2 increased dramatically (167%). As the growth rate of C also increased between P21 and P28, the growth rates of the malnourished groups lagged behind those of this group. While the growth rate of U1 was 57% to 60% of C between P35–49, the growth rate of U2 was higher than that of U1, being 71% and 87% of C (**Figure 3**).

Measurements made on P21

Rats that were malnourished between postnatal day 0 and 7 showed significantly higher values in body length, head length, 8th caudal vertebra length, left femur length, left tibia length, and ischium length compared to control rats at postnatal day 21. However, rats that were malnourished between postnatal day 14 and 21 showed significantly lower values in body length, left femur length, pelvic length, ischial length, bi-iliac width and bi-acetabular width compared to control rats. On the other hand, right humerus length and ischial width at postnatal day 21 showed no significance between all groups. When comparing the two experimental groups, all skeletal measures except right humeral length and ischial width were significantly lower in the rats malnourished in the last week of lactation than in the other group (**Table 2**).

Measurements made on P49

At the end of the 49th day, only body length, length of the left femur, bi-iliac width, bi-acetabular width, and ischial width in rats undernourished between 0–7th postnatal days showed significant deficits compared to control rats. However, rats undernourished between 14–21st postnatal days showed significant deficits in the value of body length, tail length, head width, 13th thoracic vertebra length, 8th caudal vertebra length, right humerus length, left radius length, left ulna length, left femur length, left tibia length, bi-iliac width, bi-acetabular width and ischial width compared to control rats. On the other hand, body length, tail length, 13th thoracic vertebra length, 8th caudal vertebra length, right humerus length, left radius length, left ulna length, left tibia length of rats undernourished between 14–21st postnatal

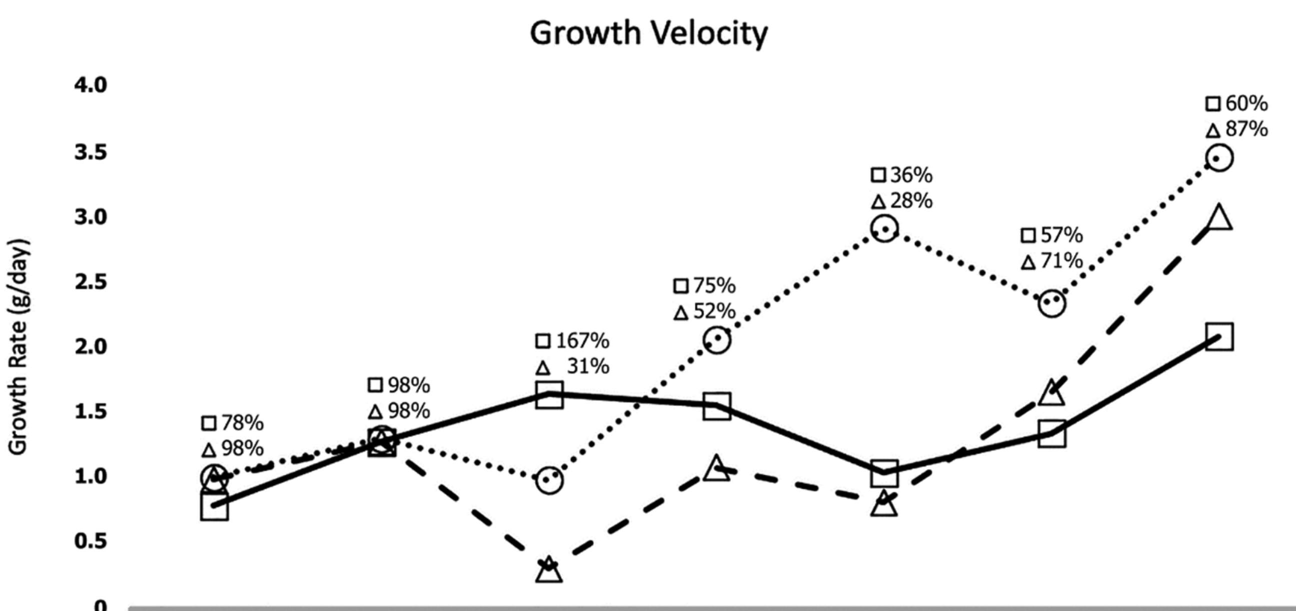

	P0-7	P7-14	P14-21	P21-28	P28-35	P35-42	P42-49
C	1.0	1.3	1.0	2.1	2.9	2.3	3.5
U1	0.8	1.3	1.6	1.6	1.0	1.3	2.1
U2	1.0	1.3	0.3	1.1	0.8	1.7	3.0

Days

Figure 3. Calculated growth rates (g/day) of the groups from day 0 (P0) to day 49 (P49), n=8. The percentages of the groups relative to the controls are given. **C:** control group; **U1:** the first group that was undernourished between day 0 (P0) and day 7 (P7); **U2:** the second group was that undernourished between day 14 (P14) and day 21 (P21).

Table 2
Measurements made from X-rays on 21st day (P21) (±standard deviation), n=8.

Measurements on P21 (cm)	C	U1	U2	Sig.
Body length	5.77±0.09	6.30±0.21	5.53±0.18	***, +, ###
Tail length	7.39±0.43	7.67±0.15	7.23±0.17	#
Head length	2.31±0.05	2.57±0.13	2.23±0.07	***, ###
Head width	1.57±0.04	1.63±0.04	1.52±0.09	##
Length of the 13. th. vertebra	0.20±0.01	0.21±0.02	0.19±0.02	#
Length of the 8. caud. vertebra	0.24±0.03	0.27±0.01	0.23±0.01	**, ###
Length of the right humerus	1.37±0.07	1.34±0.03	1.32±0.06	n.s.
Length of the left radius	1.22±0.05	1.25±0.02	1.20±0.01	#
Length of the left ulna	1.39±0.07	1.43±0.02	1.37±0.02	#
Length of the left femur	1.36±0.01	1.41±0.04	1.32±0.01	***, +, ###
Length of the left tibia	1.53±0.02	1.59±0.04	1.51±0.04	**, ###
Pelvic length	1.56±0.07	1.63±0.05	1.37±0.14	++, ###
Iliac length	0.91±0.03	0.94±0.03	0.85±0.08	##
Ischial length	0.61±0.02	0.72±0.06	0.52±0.07	**, ++, ###
Bi-iliac width	0.92±0.03	0.92±0.03	0.83±0.03	+++, ###
Bi-acetabular width	0.71±0.04	0.74±0.04	0.64±0.03	+++, ###
Ischial width	0.81±0.04	0.83±0.07	0.79±0.03	n.s.

C: control group; **U1:** the first group that was undernourished between day 0 (P0) and day 7 (P7); **U2:** the second group that was undernourished between day 14 (P14) and day 21 (P21); **sig:** significancy; ***:** comparison of C with U1; **+:** comparison of C with U2; **#:** comparison of U1 with U2. One symbol means p<0.05; two means p<0.01; three means p<0.001; **n.s.:** not significant.

days were shorter than pups undernourished in the first week of lactation. Finally, no significant difference was observed between the groups in terms of head length, pelvic length, iliac length, and ischial length measurements (**Table 3**).

Discussion

In the present study, it was observed that on the 21st postnatal day, the body weight of the pups undernourished in the last week of lactation was lower than that of the control animals, but the body weight of the pups undernourished in the first week of lactation was higher than that of the control animals due to catch-up growth. However, at the final measurements on postnatal day 49, the offspring of both undernourished groups were found to be lighter than the control animals.

Studies have shown that undernutrition in the first postnatal week reduces the body weight of infants. Winick et al.[24] undernourished their animals from P0 to P9, while Williams and Hughes[23] malnourished their rat pups from P0 to P8. Both studies reported that the body weight of these offspring was statistically lower than that of their control animals, and the statistical difference between them disappeared before the end of lactation (P0–P21).[23,24] Recent literature highlights also the significant impact of maternal undernutrition during the first week of lactation on the body weight and overall development of offspring in rat models. This critical period is essential for growth, and any nutritional deficits can lead to long-lasting effects on the progeny. Studies indicate that undernutrition during lactation can lead to stunted growth in pups. For instance, research shows that pups from mothers experiencing protein and energy restrictions during lactation exhibit minimal weight gain, contrasting sharply with those from well-nourished mothers who demonstrate rapid growth during this same period.[25,26] Specifically, one study noted that pups subjected to maternal malnutrition maintained consistent body weight during the initial week of lactation, while control groups showed significant weight increases. This discrepancy suggests that nutritional status directly influences growth trajectories in young rats.[27,28] The undernutrition period of U1 is consistent with previous studies, and the body weight of this group lagged behind that of the other groups at P7. However,

Table 3
Measurements made from X-rays on 49th day (P49) (±standard deviation), n=8.

Measurements on P49 (cm)	C	U1	U2	Sig.
Body length	9.22±0.10	9.05±0.09	8.65±0.09	**, +++, ###
Tail length	14.30±0.11	14.33±0.08	13.96±0.17	+++, ###
Head length	2.80±0.09	2.86±0.10	2.92±0.14	n.s.
Head width	1.87±0.07	1.83±0.03	1.76±0.06	+
Length of the 13th vertebra	0.30±0.01	0.29±0.02	0.26±0.01	+++, #
Length of the 8th caudal vertebra	0.63±0.02	0.66±0.06	0.54±0.04	++, ###
Length of the right humerus	1.77±0.03	1.77±0.04	1.62±0.07	+++, ###
Length of the left radius	1.60±0.07	1.58±0.04	1.44±0.05	+++, ###
Length of the left ulna	1.98±0.06	1.93±0.02	1.78±0.04	+++, ###
Length of the left femur	2.28±0.13	2.03±0.06	2.02±0.09	***, +++
Length of the left tibia	2.49±0.14	2.41±0.05	2.23±0.07	+++, ##
Pelvic length	2.40±0.28	2.49±0.12	2.36±0.12	n.s.
Iliac length	1.47±0.18	1.46±0.07	1.42±0.07	n.s.
Ischial length	0.93±0.13	1.03±0.07	0.94±0.09	n.s.
Bi-iliac width	1.48±0.10	1.34±0.03	1.28±0.04	***, +++
Bi-acetabular width	1.03±0.06	0.92±0.04	0.91±0.03	***, +++
Ischial width	1.15±0.09	1.05±0.04	0.98±0.03	*, +++

C: control group; **U1:** the first group that was undernourished between day 0 (P0) and day 7 (P7); **U2:** the second group that was undernourished between day 14 (P14) and day 21 (P21); **sig:** significancy; ***:** comparison of C with U1; **+:** comparison of C with U2; **#:** comparison of U1 with U2. One symbol means $p<0.05$; two means $p<0.01$; three means $p<0.001$; **n.s.:** not significant.

unlike the above studies, U1 did not catch up between P7 and P14. Instead, U1 showed this period of accelerated growth between P14 and P21, exceeding the growth rate of C by 67%. This late catch-up period may be due to insufficient maternal milk production immediately after malnutrition. However, strain differences could also be a factor in the occurrence of differences in this recovery phase. Also, the composition of maternal milk is crucial for pup development. Research indicates that malnourished mothers may produce milk with lower macronutrient levels, which could further exacerbate growth issues in their offspring.[29,30] Although some studies did not find significant differences in protein or fat content between milk from malnourished and control dams, there is evidence suggesting that bioactive factors in milk may play a role in modulating growth outcomes.[29] The catch-up growth period observed in other studies peaked at P21[23,31,32] and it can be seen that the growth rate of U1 slowed down after seven days, so that the body weight of U1 at P28 is no longer different from that of C.

In our study, the U2 pups did not show a steep catch-up process like the pups from U1. But after P28, a steady accelerated growth was observed compared to U1. There are no studies that we can directly compare to the period of undernutrition of U2. In contrast to our observations some Studies indicate that pups from mothers experiencing undernutrition during the third week of lactation exhibit accelerated weight gain compared to control groups. This catch-up growth is observed as pups begin consuming solid food in addition to suckling maternal milk.[29,33] But a study on early weaning could lead to similar results. Pietrobon et al.[34] pharmacologically or physically inhibited offspring milk intake during the last three days of breastfeeding. Body weight of malnourished males still lagged behind that of the control group at P45 (although there was no statistical difference). However, at P150, the body weight of the experimental groups exceeded that of the control group. The authors concluded that early weaning caused metabolic changes in the experimental groups.[34] While the data from this study up to P45 are consistent with our study, we do not know if the results at P150 are the same for us. However, the argument made by the authors for the cause of growth retardation in the subjects could also apply to our subjects.

The body weights and growth rates of our experimental groups decreased from P28 to P35. This suggests that the offspring in the experimental groups have not completed their development and therefore cannot feed sufficiently independently. Ferraz-Perreira et al.[35] suggested that malnutrition reduces masticatory efficiency by slowing, weakening and delaying the maturation of masticatory muscles. However, in another study, perinatal undernutrition was observed to reduce the number of taste buds in rats.[36] Both arguments could explain why undernourished rats develop less than control subjects immediately after weaning.

The final body weights measured at puberty showed that the weights of the experimental groups were still lower than those of the control group, but the difference between the experimental groups was closed. Williams et al.[32] reported that the weight losses of malnourished rats continued after P120.[32] However, it was observed that although the malnourished rats consumed 30% more food than their control counterparts after the nutritional insult. These animals ate more irregularly and less food than the control animals in the following days.[22] Williams and Hughes[23] found in their study that the effects of malnutrition were greater in the late stages of lactation. However, the animals in this study were undernourished in three different groups from birth to P8, P14 and P21. The offspring that were malnourished from P0 to P8 reached the control group at P22. In contrast, the other two groups already had lower body weights at P120.[23] The body weights of the undernourished pups during lactation were lower at P21 and remained lower at P150.[37] Recent studies indicate that maternal undernutrition can alter hormonal profiles and neuropeptide expressions related to appetite regulation in offspring. This alteration may lead to increased caloric intake but decreased fat storage efficiency, resulting in abnormal growth patterns as seen in various studies.[25,30] Despite the nutritional restoration through adequate calories later in life, the capacity for catch-up growth is diminished in pups subjected to maternal undernutrition during the third week of lactation. This suggests that early-life nutritional deficits can have lasting effects on growth trajectories.[38] Since the results of our study showed that the body weight of U1 was higher than that of U2 at P28, P35 and P42, this suggests that the 3rd week of lactation is a more critical postnatal developmental period.

Our measurements immediately after weaning showed that although the measurements of U1 were higher than those of the other groups due to catch-up growth, the size of the thoracic vertebrae was not affected. However, measurements at P49 showed that both the thoracic and caudal vertebrae of U2 were less developed than the other two groups, suggesting that malnutrition in the last week of lactation affects vertebral size in the long term. This suggestion is also supported by the shorter tail length of U2. Research supports our observations and states that undernutrition during lactation can lead to significant reductions in vertebral size and integrity. Studies have shown that malnutrition during lactation can lead to a significant reduction in the size and integrity of the spine. Puppies from malnourished mothers have smaller vertebrae compared to those from well-nourished mothers, probably due to insufficient calcium and protein intake.[39] A more recent study confirms this opinion by finding that puppies from malnourished mothers have smaller vertebrae than those from well-nourished mothers. And that this reduction is often due to inadequate calcium and protein intake, which are essential for bone growth and density.[40] Based on our observations on U2, we can assume that the last week of lactation is a critical period for vertebral development. Several studies indicate that pups from mothers experiencing undernutrition during lactation exhibit reduced body length compared to control groups. This effect is observed throughout the lactation period and into adulthood.[29,41] Despite the nutritional restoration through adequate calories after weaning, the capacity for catch-up growth in body length is often diminished in pups subjected to maternal undernutrition during lactation. Even when body weight normalizes, linear growth deficits may persist.[41] In a study of protein restriction during pregnancy, short spines were reported in protein-restricted rats.[42] In a more recent study, Nemoto and Kakinuma[43] fed dams a calorie-restricted diet during pregnancy and reported that the pups failed to catch up and resulted in short body length.[43]

Dahinten and Pucciarelli[44] observed in their study of rats that prenatal malnutrition affects many cranial parameters. However, this study concludes that postnatal malnutrition has a greater negative effect on these parameters.[44] This may be attributed to the fact that 85% of cortex neurogenesis in the rat occurs after birth.[45] Although U1 had a rapid growth curve before P21, the cranial width of U1 was not different from that of C at P49. On postnatal day 21, the skull length of pups malnourished between 0–7 days of the lactation period was greater than that of the control group; however, this difference disappeared on postnatal day 49. In contrast to the U1 pups, the U2 pups had a smaller head width at postnatal day 49. In a previous study, the deficit in this parameter persisted until 200 days of age in rats that were malnourished from gestation day 18 to 100 days of age.[22] Recent studies are in line with our observations. They indicate that pups from mothers experiencing undernutrition during lactation exhibit reduced skull size compared to control groups. This effect is observed in various cranial measurements, including skull length, width, and height.[46–48] It is also emphasized that maternal undernutrition during lactation can lead to changes in the shape of the skull. One study found that the skulls of pups from undernourished mothers were smaller and thinner than those of the control group in several parameters.[48]

At 21 days of age, the body length, the length of the 8th caudal vertebra, the length of the left femur, the length of the left tibia, and the length of ischial bones were longer in U1 than in the control animals, while the pups of the U2 group had smaller skeletons than the control animals. At 49 days of age, the significant differences in some features of the skeleton between U1 and control rats disappeared except for femur length. However, some features of the pelvic bones of the U1 rats differed from those of the control animals. In contrast to the U1 rats, the U2 rats had smaller skeletal measurements than the control rats at 49 days of age, except for pelvic bone lengths and head length.

Research has demonstrated that undernutrition during lactation leads to significant reductions in pelvic size and dimensions in offspring. For instance, pups from undernourished mothers exhibit smaller pelvic widths and lengths compared to those from well-nourished controls. This reduction can have implications for reproductive health and overall mobility in adulthood.[38,49] It was found that the rat pelvis develops rapidly from P0 to P80, that ossification of the acetabular complex begins at P70, and that synostosis of the three pelvic components begins at P100.[50] Therefore, the effects of nutrition can be observed directly on the rat pelvis because the pelvic components are not fully developed on the days of the measurements. Studies of malnutrition have shown that pelvic dimensions do not recover despite a prolonged period of rehabilitation.[29,33,51] Although the measurements we performed on P49 confirm this study, they emphasize that undernutrition even in only a part of lactation affects the measurements of pelvic widths of pups and may cause permanent damage.

Our study shows that undernutrition in either the first or last week of the lactation period affects long bone development. In particular, U2 measurements are similar to limb measurements of offspring malnourished prenatally or throughout the lactation period. This observation suggests that especially the last week of lactation is a critical period for long bone development.

Nakamoto and Miller[52] have reported that long bones are more prone to malnutrition.[52] According to Kimura et al.,[53] prenatal malnutrition impairs postnatal growth of the tibia.[53] It was observed that postnatally malnourished rats showed catch-up growth after weaning, but their tibial length remained shorter than that of the control group even at week 15.[54] Numerous studies have reported that undernutrition during lactation results in significantly reduced length and density of long bones, such as the femur and tibia. For example, research by Babinski et al.[38] demonstrated that pups from mothers on low-protein diets exhibited stunted growth in femoral length and altered bone density compared to those from well-nourished mothers. This reduction is attributed to inadequate intake of essential nutrients, particularly protein and calcium, which are vital for bone development.[38] The timing and rate of bone growth are also affected by maternal nutrition. A study by Ortiz-Valladares et al.[49] indicated that while long bone measurements may not show immediate deficits, the growth trajectories are altered, resulting in delayed skeletal maturation in pups subjected to undernutrition. This delayed growth can have long-term implications, as it may affect the overall structural integrity of the bones as the rats reach adulthood.[49] The effects of maternal undernutrition during lactation can persist into adulthood, with previously undernourished rats exhibiting altered long bone morphology. Studies indicate that even after nutritional rehabilitation post-weaning, these rats may continue to show reduced bone length and density, potentially increasing their risk for fractures and other skeletal issues later in life.[38]

Conclusion

The results of our study showed that undernutrition in the first or last week of lactation can cause long-term damage to body weight and pelvic measurements of rats. However, most skeletal measurements of rats exposed to undernutrition in the last week of lactation were lower than those of the control group and the group exposed to undernutrition in the first week of lactation. These results suggest that the last week of lactation is more critical for skeletal development.

Conflict of Interest

The authors declare that they have no known conflicts of interest.

Author Contributions

HA: investigation, data curation, software, writing- original draft; FY: methodology, resources, supervision, writing - review & editing.

Ethics Approval

All animal applications in this study were approved by the local ethics committee of Eskişehir Osmangazi University (protocol number 155/850).

Funding

No funding were used for this study.

References

1. 2022 Global Nutrition Report. [Internet]. [Retrieved on April 28, 2024]. Available from: https://globalnutritionreport.org/reports/2022-global-nutrition-report/
2. 2021 Global Nutrition Report. [Internet]. [Retrieved on April 28, 2024]. Available from: https://media.globalnutritionreport.org/documents/2021_Global_Nutrition_Report_aUfTRv0.pdf.
3. Kakaei H, Nourmoradi H, Bakhtiyari S, () Effect of COVID-19 on food security, hunger, and food crisis. In: COVID-19 and the Sustainable Development Goals. Elsevier, 2022, pp. 3–29.
4. 2021 Global Report on Food Crises reveals scope of food crises as COVID-19 poses new risks to vulnerable countries. [Internet]. [Retrieved on April 20, 2024]. Available from: https://www.unicef.org/turkiye/en/press-releases/global-report-food-crises-reveals-scope-food-crises-covid-19-poses-new-risks
5. 2022 COVID-19 Brief: impact on food security. [Internet]. [Retrieved on April 20, 2024]. Available from: https://www.usglc.org/coronavirus/global-hunger/#:~:text=In%202022%2C%20COVID%2D19%20disruptions,drought%2C%20and%20the%20Ukraine%20crisis
6. 2021 Food and nutrition under the COVID-19 crisis: lessons for protecting the vulnerable and facilitating recovery. [Internet]. [Retrieved on April 11, 2024]. Available from: https://ieg.worldbankgroup.org/sites/default/files/Data/Topic/COVID19Lessons_foodandnutrition.pdf
7. 2020 Policy brief: the impact of COVID-19 on food security and nutrition. [Internet]. [Retrieved on April 12, 2024]. Available from: https://unsdg.un.org/resources/policy-brief-impact-covid-19-food-security-and-nutrition
8. Media - nutrition international. [Internet]. [Retrieved on April 12, 2024]. Available from: https://www.nutritionintl.org/media/
9. Ahmed MGE, Bedi KS, Warren MA, Kamel MM. Effects of a lengthy period of undernutrition from birth and subsequent nutritional rehabilitation on the synapse: granule cell neuron ratio in the rat dentate gyrus. J Comp Neurol 1987;263:146–58.
10. Angulo-Colmenares AG, Vaughan DW, Hinds JW. Rehabilitation following early malnutrition in the rat: body weight, brain size, and cerebral cortex development. Brain Res 1979;169:121–38.
11. Barnes D, Altman J. Effects of different schedules of early undernutrition on the preweaning growth of the rat cerebellum. Exp Neurol 1973;38:406–19.
12. Barnes D, Altman J. Effects of two levels of gastational-lactational undernutrition on the postweaning growth of the rat cerebellum. Exp Neurol 1973;38:420–8.
13. Yücel F, Akgün Z, Eğilmez H, Solak O. Effects of undernutrition and rehabilitation on the skeletal growth of rats. Turkish Journal of Medical Sciences 1996;26:231–6.
14. Bedi KS, Hall R, Davies CA, Dobbing J. A stereological analysis of the cerebellar granule and purkinje cells of 30-day-old and adult rats undernourished during early postnatal life. J Comp Neurol 1980;193:863–70.
15. Bedi KS, Thomas YM, Davies CA, Dobbing J. Synapse-to-neuron ratios of the frontal and cerebellar cortex of 30-day-old and adult rats undernourished during early postnatal life. J Comp Neurol 1980;193:49–56.
16. Clos J, Favre C, Selme-Matrat M, Legrand J. Effects of undernutrition on cell formation in the rat brain and specially on cellular composition of the cerebellum. Brain Res 1977;123:13–26.
17. Fish I, Winick M. Effect of malnutrition on regional growth of the developing rat brain. Exp Neurol 1969;25:534–40.
18. Spanheimer R, Zlatev T, Umpierrez G, DiGirolamo M. Collagen production in fasted and food-restricted rats: response to duration and severity of food deprivation. J Nutr 1991;121:518–24.
19. Hughes PC, Tanner JM. The assessment of skeletal maturity in the growing rat. J Anat 1970;106:371–402.
20. Hughes PC. Catch-up growth in the limbs of rats undernourished for different lengths of time during suckling. Acta Anat (Basel) 1986;125:50–8.
21. Jones DG, Dyson SE. Synaptic junctions in undernourished rat brain—an ultrastructural investigation. Exp Neurol 1976;51:529–35.
22. Warren MA, Bedi KS (1985) The effects of a lengthy period of undernutrition on the skeletal growth of rats. J Anat 141:53–64
23. Williams JP, Hughes PC. Catch-up growth in rats undernourished for different periods during the suckling period. Growth 1975;39: 179–93
24. Winick M, Fish I, Rosso P. Cellular recovery in rat tissues after a brief period of neonatal malnutrition. J Nutr 1968;95:623–6.
25. Passos MCF, Ramos CF, Moura EG. Short and long term effects of malnutrition in rats during lactation on the body weight of offspring. Nutrition Research 2000;20:1603–12.
26. Pessoa DC, Lago ES, Teodósio NR, Bion FM. Dietary proteins on reproductive performance in three consecutive generations of rats. Arch Latinoam Nutr 2000;50:55–61.
27. Cambraia RPB, Vannucchi H, Almeida SS, De-Oliveira LM. Effects of malnutrition during early lactation on development and feeding behavior under the self-selection paradigm. Nutrition 2001;17:455–61.
28. Rasmussen KM. Effects of under- and overnutrition on lactation in laboratory rats. J Nutr 1998;128:390S–3S.
29. Rodríguez-Rodríguez P, Monedero-Cobeta I, Ramiro-Cortijo D, Puthong S, Quintana-Villamandos B, Gil-Ramirez A, Canas S, Ruvira S, Arribas SM. Slower growth during lactation rescues early cardiovascular and adipose tissue hypertrophy induced by fetal undernutrition in rats. Biomedicines 2022;10:2504.
30. Vargas R, Martins IP, Matiusso CCI, Casagrande RA, Zara CB, Huppes de Souza AC, Horst WP, Sieklicki TC, Becker TCA,

Lucredi NC, Comar JF, Malta A, Mathias PCF. Protein restriction during lactation causes transgenerational metabolic dysfunction in adult rat offspring. Front Nutr 2023;9:1062116.

31. Hughes PC. Catch-up growth in the limbs of rats undernourished for different lengths of time during suckling. Acta Anat (Basel) 1986;125:50–8.
32. Williams JPG, Tanner JM, Hughes PCR. Catch-up growth in male rats after growth retardation during the suckling period. Pediatr Res 1974;8:149–56.
33. Léonhardt M, Lesage J, Croix D, Dutriez-Casteloot I, Beauvillain JC, Dupouy JP. Effects of perinatal maternal food restriction on pituitary-gonadal axis and plasma leptin level in rat pup at birth and weaning and on timing of puberty. Biol Reprod 2003;68:390–400.
34. Pietrobon CB, Bertasso IM, Silva BS, Peixoto-Silva N, Oliveira E, Moura EG, Lisboa PC. Body adiposity and endocrine profile of female wistar rats of distinct ages that were early weaned. Horm Metab Res 2020;52:58–66.
35. Ferraz-Pereira KN, Da Silva Aragão R, Verdier D, Toscano AE, Lacerda DC, Manhães-de-Castro R, Kolta A. Neonatal low-protein diet reduces the masticatory efficiency in rats. Br J Nutr 2015; 114:1515–30.
36. Salas M, Rubio L, Torrero C, Carreon M, Regalado M. Effects of perinatal undernutrition on the circumvallate papilla of developing Wistar rats. Acta Histochem 2016;118:581–587.
37. Vicente LL, De Moura EG, Lisboa PC, Monte Alto Costa A, Amadeu T, Mandarim-de-Lacerda CA, Passos MC. Malnutrition during lactation in rats is associated with higher expression of leptin receptor in the pituitary of adult offspring. Nutrition 2004;20: 924–8.
38. Babinski MSD, Ramos CF, Fernandes RMP, Cardoso GP, Babinski MA. Maternal malnutrition diet during lactation period leads to incomplete catch-up growth in femur of the pups at adulthood. Int J Morphol 2016;34:71–7.
39. Lobe SL, Bernstein MC, German RZ. Life-long protein malnutrition in the rat (Rattus norvegicus) results in altered patterns of craniofacial growth and smaller individuals. J Anat 2006;208:795–812.
40. Argov-Argaman N, Altman H, Janssen JN, Daeem S, Raz C, Mesilati-Stahy R, Penn S, Monsonego-Ornan E. Effect of milk fat globules on growth and metabolism in rats fed an unbalanced diet. Front Nutr 2024;10:1270171.
41. Reichling TD, German RZ. Bones, muscles and visceral organs of protein-malnourished rats (Rattus norvegicus) grow more slowly but for longer durations to reach normal final size. J Nutr 2000; 130:2326–32.
42. Shrader RE, Zeman FJ. Skeletal development in rats as affected by maternal protein deprivation and postnatal food supply. J Nutr 1973;103:792–801.
43. Nemoto T, Kakinuma Y. Fetal malnutrition-induced catch up failure is caused by elevated levels of miR-322 in rats. Sci Rep 2020; 10:1339.
44. Dahinten SL, Pucciarelli HM. Effects of protein-calorie malnutrition during suckling and post-weaning periods on discontinuous cranial traits in rats. Am J Phys Anthropol 1983;60:425–30.
45. Altman J, Bayer SA. Migration and distribution of two populations of hippocampal granule cell precursors during the perinatal and postnatal periods. J Comp Neurol 1990;301:365–81.
46. Barbeito-Andrés J, Gonzalez P, Hallgrímsson B. Prenatal development of skull and brain in a mouse model of growth restriction. Revista Argentina de Antropologia Biologica 2016;18:1–13.
47. Fernandes RM, Abreu AV, Silva RB, Silva DF, Martinez GL, Babinski MA, Ramos CF. Maternal malnutrition during lactation reduces skull growth in weaned rat pups: experimental and morphometric investigation. Anat Sci Int 2008;83:123–30.
48. Pires L, Junior A, Chagas C, Manaia JHM, Gameiro VS, Babinski MA. Maternal undernutrition during lactation leads to reduction in skull size and thickness of adult-aged Wistar rats. Arch Med Sci 2020;17:1093–9.
49. Ortiz-Valladares M, Salcedo, CA, Ortega MR, Solorio CT, Alvarado MS. Long-term alterations on the physical development of pre- and neonatally undernourished Wistar rats: a functional correlation. Neurobiología Revista Electronica 2019;10:1–14
50. Dixon AD, Gakunga PT. Morphometric changes in growth of the rat pelvis after papain administration. Anat Rec 1993;235:312–8.
51. Dickerson JWT, Hughes PCR, McAnulty PA. The growth and development of rats given a low-protein diet. Br J Nutr 1972;27: 527–536.
52. Nakamoto T, Miller SA. Physical and biochemical changes of the mandible and long bone in protein-energy malnourished newborn rats. J Nutr 1979;109:1477–82.
53. Kimura T, Hino K, Kono T, Takano A, Nitta N, Ushio N, Hino S, Takase R, Kudo M, Daigo Y, Morita W, Nakao M, Nakatsukasa M, Tamagawa T, Rafiq AM, Matsumoto A, Otani H, Udagawa J. Maternal undernutrition during early pregnancy inhibits postnatal growth of the tibia in the female offspring of rats by alteration of chondrogenesis. Gen Comp Endocrinol 2018;260:58–66.
54. Prior LJ, Velkoska E, Watts R, Cameron-Smith D, Morris MJ. Undernutrition during suckling in rats elevates plasma adiponectin and its receptor in skeletal muscle regardless of diet composition: a protective effect? Int J Obes (London) 2008;32:1585–94.

ORCID ID:
H. Ay 0000-0003-4638-0750;
F. Yücel 0000-0002-1238-1483

Correspondence to: Hakan Ay, PhD, Assist. Prof.
Department of Anatomy, Faculty of Medicine,
Eskişehir Osmangazi University, Eskişehir, Türkiye
Phone: +90 222 239 29 79 / 4431
e-mail: hakanay@ogu.edu.tr

deomed

Conflict of interest statement: No conflicts declared.

 How to cite this article: Ay H, Yücel F. Undernutrition in the last period of lactation may have adverse effects on skeletal development. Anatomy 2024;18(3):91–100.

Original Article

http://dergipark.org.tr/en/pub/anatomy
Received: October 2 2024; Accepted: December 24, 2024
doi:10.2399/ana.24.1594501

anatomy
An International Journal of Experimental and Clinical Anatomy

The impact of laterality on the morphometric angular features of the scapula

Seda Sertel Meyvacı[1], Handan Ankaralı[2], Beyza Çelik[1]

[1]*Department of Anatomy, Faculty of Medicine, Bolu Abant İzzet Baysal University, Bolu, Türkiye*
[2]*Department of Anatomy, Faculty of Medicine, Istanbul Medeniyet University, Istanbul, Türkiye*

Abstract

Objectives: This study aimed to analyze the angular measurements and morphological characteristics of the scapula, providing insights to enhance surgical interventions and clinical research requiring detailed anatomical knowledge, such as total shoulder arthroplasty, fracture fixation via screw placement, and scapular arthroscopic procedures.

Methods: Twenty dry scapula (13 right, 7 left) of unknown age and sex, obtained from the bone archive of the Anatomy Department at Bolu Abant İzzet Baysal University Faculty of Medicine, were analyzed. Angular measurements were conducted using a digital angle gauge. Due to the limited sample size, normality testing was not performed. Statistical comparisons between the right and left scapula were made using the Mann-Whitney U test, with a significance level set at $p \leq 0.05$.

Results: Among the six angular parameters measured, only the lateral angle demonstrated a statistically significant difference between the right and left sides ($p=0.033$).

Conclusion: The findings indicate that, except for the lateral angle, the scapula's angular measurements are predominantly symmetrical between the right and left sides. The glenoid profile angle (GPA) may serve as a valuable marker for assessing fracture risk in the glenoid fossa, aiding orthopedic surgeons in clinical decision-making. A detailed understanding of scapular morphology is expected to advance both surgical practices and anatomical research.

Keywords: angular assesment; forensic anthropology; scapula morphometry; Turkish population

Anatomy 2024;18(3):101–105

Introduction

The scapula, a critical component of the pectoral girdle, features a distinct irregular, flat triangular shape with two primary surfaces: the costal (anterior) surface and the dorsal (posterior) surface. The dorsal surface is characterized by the scapular spine, which divides it into the supraspinous fossa and infraspinous fossa. This spine originates medially and extends laterally to culminate at the acromion. The scapula also includes three borders—superior, medial (vertebral), and lateral (axillary)—and three angles formed at the junctions of these borders: the superior, inferior, and lateral angles. The superior angle, situated at the intersection of the superior and medial borders, aligns with the second rib and serves as the attachment site for the levator scapula muscle. The inferior angle, where the medial and lateral borders converge, is located at the level of the seventh rib or seventh intercostal space and provides an attachment point for the serratus anterior muscle. The lateral angle, the thickest portion of the scapula, houses the glenoid fossa, the articulation site for the humeral head. These anatomical landmarks significantly influence the musculature associated with the scapula, underscoring its pivotal role in shoulder girdle movement and its clinical relevance.[1,2]

Scapular fractures, although rare, account for 3–5% of shoulder girdle injuries and less than 1% of all fractures.[3] Among these, the glenopolar angle (GPA) is of particular clinical importance in scapular neck fractures. The GPA, which quantifies the glenoid's inclination relative to the scapular body on an anteroposterior plane, typically ranges between 36° and 43° in healthy individuals. Values outside this range, such as a GPA of 20°–22°, often indicate a need for surgical intervention to prevent long-term complications, including pain, weakness, and impaired daily activities.[4–7]

Bestard et al.[8] were the first to establish the standard GPA range of 30°–45°, identifying deviations as indicators of scapular neck fracture dysplasia. Furthermore, Labler et al.[9] recommended surgical treatment when the GPA falls below 3°, as this suggests potential ligament rupture Kim et al.[10] emphasized the GPA's role in both the planning and postoperative evaluation of floating shoulder treatments.

The objective of this study is to analyze the angular measurements and morphological characteristics of the scapula, contributing to the anatomical knowledge required for surgical procedures and clinical research, including scapular arthroscopic interventions.

Materials and Methods

Measurements were obtained using a digital angle gauge from 20 dry scapula (13 right, 7 left) of unknown sex and age, sourced from the bone archive of the Anatomy Department at Bolu Abant İzzet Baysal University School of Medicine. The specific morphometric measurements performed on the scapula are as follows and are illustrated in **Figure 1**:

- **Inferior Angle (AI):** The angle formed between the medial and lateral borders of the scapula.
- **Superior Angle (AS):** The angle formed between the medial and superior borders of the scapula.
- **Lateral Angle (AL):** The angle formed between the lateral and superior borders of the scapula.
- **MSU:** The angle between the portion of the medial border above the scapular spine and the spine itself.
- **MSA:** The angle between the portion of the medial border below the scapular spine and the spine itself.
- **Glenopolar Angle (GPA):** The angle between the axis passing through the supraglenoid and infraglenoid tubercules, and the axis drawn from the apex of the supraglenoid tubercle to the most caudal point of the scapular body.

Descriptive statistics for the collected data included mean±standard deviation, median, quartiles, minimum, and maximum values for numerical measurements. Categorical variables were analyzed as percentages (%). Due to the limited sample size, normality testing was not conducted, and comparisons between right and left scapula were performed using the Mann-Whitney U test. Statistical analysis was conducted using SPSS for Windows, version 29.0 (IBM, Armonk, NY, USA). A significance level of $p<0.05$ was considered statistically significant.

Results

The results of the comparison between the measurements of the right and left scapula are summarized in **Table 1**. And **Table 2** presents the descriptive statistics of angular measurements for all 20 scapula combined, without differentiating between the right and left sides. The results suggested that the lateral angle (AL) is significantly greater on

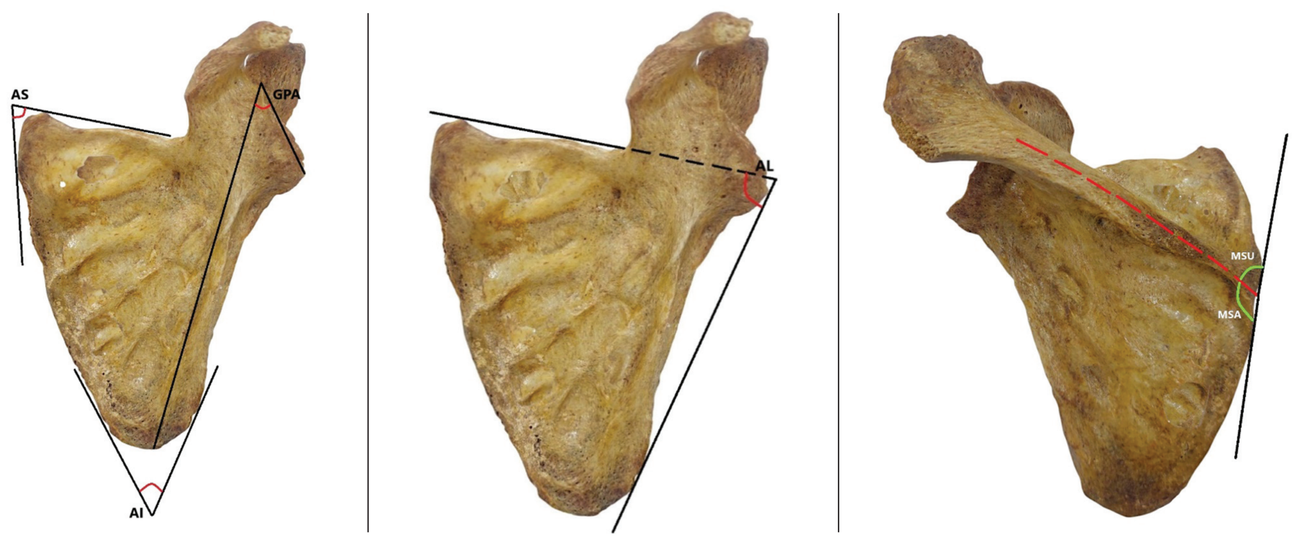

Figure 1. Illustration of scapular measurements on dry scapula. AI: The angle formed between the medial and lateral borders; AS: the angle formed between the extended lines of the medial and superior borders; AL: the angle formed between the lateral and superior borders; MSA: the angle between the portion of the medial border below the scapular spine and the spine itself; MSU: the angle between the portion of the medial border above the scapular spine and the spine itself; GPA: the angle between the axis passing through the supraglenoid and infraglenoid tubercules, and the axis drawn from the apex of the supraglenoid tubercle to the most caudal point of the scapular body.

Table 1
Comparison of angular measurements between right and left scapula.

		n	Mean±SD	95% confidence interval for mean Lower bound	95% confidence interval for mean Upper bound	Min	Max	p-value
AI	Left	7	68.57±13.30	56.27	80.87	48	87	0.393
	Right	13	63.46±6.42	59.58	67.34	50	72	
AS	Left	7	78.29±6.73	72.07	84.51	68	85	0.485
	Right	13	76.38±5.72	72.93	79.84	69	88	
AL	Left	7	81.43±3.50	78.19	84.67	76	87	**0.046**
	Right	13	76.38±5.12	73.29	79.48	69	85	
MSU	Left	7	67.86±8.97	59.56	76.15	57	82	0.211
	Right	13	62.54±8.48	57.41	67.66	53	84	
MSA	Left	7	107.86±6.84	101.53	114.18	97	117	0.643
	Right	13	106.77±7.79	102.06	111.48	94	125	
GPA	Left	7	38.00±3.65	34.62	41.38	32	43	0.097
	Right	13	34.23±4.95	31.24	37.22	27	44	

AI: The angle formed between the medial and lateral borders; **AS:** the angle formed between the extended lines of the medial and superior borders; **AL:** the angle formed between the lateral and superior borders; **max:** maximum; **min:** minimum; **MSA:** the angle between the portion of the medial border below the scapular spine and the spine itself; **MSU:** the angle between the portion of the medial border above the scapular spine and the spine itself; **GPA:** the angle between the axis passing through the supraglenoid and infraglenoid tubercules, and the axis drawn from the apex of the supraglenoid tubercle to the most caudal point of the scapular body.

the left side ($p<0.05$). However, no significant differences were observed between the right and left sides for the remaining five angular parameters, indicating a high degree of symmetry in these measurements.

Discussion

The scapula, a key structure of the pectoral girdle, is characterized by its triangular shape, three borders, and three angles formed by the intersection of these borders.[1] The spine of the scapula divides the dorsal surface into the supraspinous and infraspinous fossae, which serve as attachment sites for several muscles. Functionally, the scapula articulates with the clavicle and humerus, facilitating shoulder girdle movements, and is therefore of critical clinical importance.[2] In this study, six angular parameters of the scapula were measured, and their symmetry between the right and left sides was evaluated. Among these parameters, only the AL exhibited a statistically significant difference between the two sides ($p=0.033$). The mean values for the parameters were as follows: AS:

Table 2
Summary of average angular measurements for right and left scapula.

		n	Mean±SD	95% confidence interval for mean Lower bound	95% confidence interval for mean Upper bound	Min	Max
General	AI	20	65.25±9.39	60.85	69.65	48	87
	AS	20	77.05±5.99	74.25	79.85	68	88
	AL	20	78.15±5.15	75.74	80.56	69	87
	MSU	20	64.40±8.81	60.28	68.52	53	84
	MSA	20	107.15±7.31	103.73	110.57	94	125
	GPA	20	35.55±4.81	33.30	37.80	27	44

AI: The angle formed between the medial and lateral borders; **AS:** the angle formed between the extended lines of the medial and superior borders; **AL:** the angle formed between the lateral and superior borders; **max:** maximum; **min:** minimum; **MSA:** the angle between the portion of the medial border below the scapular spine and the spine itself; **MSU:** the angle between the portion of the medial border above the scapular spine and the spine itself; **GPA:** the angle between the axis passing through the supraglenoid and infraglenoid tubercules, and the axis drawn from the apex of the supraglenoid tubercle to the most caudal point of the scapular body.

77.05°±6, AI: 65.25°±9.4, AL: 78.15°±5.15, MSU: 64.4°±8.81, MSA: 107.15°±7.31, and GPA: 35.55°±4.81. These findings provide insights into scapular morphology and its implications for clinical and surgical applications.

Measurements of the superior angle have been studied in various populations, highlighting notable differences. Piyawinijwong et al.,[11] in their research on the Thai population, reported a mean value of 84.29°±9.43. Similarly, Sanga[12] determined the superior angle to be 89.57°±10.47 in the Indian population, while Zhang et al.[13] calculated an average value of 88.72° in their analysis of three superior angle types within the Chinese population. In a study of the Turkish population, Boyan et al.[14] identified a mean value of 95.5°, categorizing the scapula into six types based on the structure of the suprascapular notch. Notably, the value measured in our study (77.05°±6) is considerably lower than these findings.

Regarding the inferior angle, our study measured a mean value of 65.25°±9.4, which closely aligns with the findings of Boyan et al.[14] However, lower values were observed in other studies, with Piyawinijwong et al.[11] reporting 40.88°±5.29 and Sanga[12] noting 44.85°±8.14. The lateral angle in our study showed a statistically significant difference between the right and left sides (left: 81.43°±3.505, right: 76.38°±5.12). This is notably higher compared to the findings of Sanga,[12] who reported a lateral angle of 62.38°±10.05. The GPA a critical parameter for evaluating the glenoid slope relative to the scapular body, typically ranges between 36° and 43° in healthy individuals.[4] It is clinically significant, with values between 20° and 22° often indicating the need for surgical intervention to prevent long-term complications such as pain, weakness, and impaired daily function.[5–7]

Bestard et al.[8] first established the standard glenopolar angle (GPA) as ranging from 30° to 45°, highlighting values outside this range as critical indicators of dysplasia in scapular neck fractures Pazarcı et al.[15] compared GPA values between patients with anterior shoulder dislocation (Group 1) and a control group (Group 2), found averages of 32.34°±1.96 and 34.50°±2.32, respectively, noting a statistically significant difference but no gender-based variation. Similarly, Cini et al.[16] calculated a GPA of 38.6°±4.54 and proposed a regression formula for its estimation Sanga[12] reported a GPA of 38.65°±5.66° in dry scapula.

Kumari et al.[17] conducted a morphological analysis of GPA in the Indian population and found an average GPA of 42.6° for all scapula, with no significant differences between sides. They also demonstrated variance among measurement techniques: 42.6° from dry scapula, 39.8° from AP radiological images, and 42.3° from Neer I view radiographs. Pace et al.[18] found a GPA of 39° (ranging from 26° to 50°) in AP radiographs of 9 patients. Tuček et al.[19] further demonstrated method-dependent variation in GPA values: 42.3°±1.6 in 100 dry scapula, 37.1°±4.9 in 50 AP chest radiographs, 35.9° in 50 AP shoulder radiographs, and 43.0°±1.4 in 3D CT reconstructions. In our study, the mean GPA was 35.55°±4.81, aligning with lower values reported in studies involving radiological imaging. The discrepancies between measurements obtained from radiological images and dry bones emphasize the impact of measurement techniques on GPA outcomes.[9,16,18,19] Additionally, variations in GPA may be influenced by anatomical structures like the supraglenoid and infraglenoid tubercles, which serve as attachment points for the biceps brachii and triceps brachii muscles.[20]

Our findings provide valuable data on scapular morphometry in the Turkish population. The results suggest that angular characteristics of the scapula are generally symmetrical between the right and left sides, except for the lateral angle, which showed a statistically significant difference. These findings underscore the importance of further research, particularly on lateral angle variation. Limitations of our study include a small sample size and the absence of gender-specific data, which restrict the generalizability of our results. Future studies with larger, demographically diverse samples and comparisons across measurement techniques, including radiological imaging and 3D modeling, are anticipated to significantly enrich the literature.

Conclusion

This study offers valuable insights into the morphometric characteristics of the scapula in the Turkish population. While the scapula generally exhibits a symmetrical structure between the right and left sides, the observed differences in the lateral angle underscore the need for further research in this area. The GPA measurements, in particular, demonstrate clinical utility for applications such as fracture management and assessing dysplasia. However, the study's limitations—including a small sample size and the absence of gender-specific analysis—restrict the broader applicability of the findings. Future research involving larger and more demographically balanced sample groups is essential to enhance the robustness of the results. Additionally, comparing different measurement techniques, such as radiological imaging and 3D modeling, is anticipated to yield significant contributions to the literature, providing a more comprehensive understanding of scapular anatomy and its clinical implications.

Acknowledgment

We are deeply grateful to the body donors and their families for their generous contributions, which made this study possible and significantly supported scientific research and education.

Conflict of Interest

There is no conflict of interest among the authors regarding the publication of this manuscript.

Author Contributions

SSM: project development, literature review, manuscript writing, critical revision of the text, design and planning of the method; HA: data analysis, manuscript editing, critical revision of the text, design and planning of the method; BÇ: data collection, literature review, manuscript writing, editing of the text.

Ethics Approval

Ethical approval was received from Bolu Abant İzzet Baysal University, Non-Interventional Clinical Researches Ethics Committee Approval for the present study with decision number: 2024/339.

Funding

There is no financial support for this manuscript.

References

1. Standring S. Gray's anatomy: the anatomical basis of clinical practice. 42nd ed. Edinburgh (Scotland): Elsevier Churchill Livingstone; 2020. p. 1606.
2. Kabakcı AG, Polat S, Yücel AH. Morphometric analysis and clinical significance of scapula. [Article in Turkish] Cukurova Medical Journal 2019;44:788–93.
3. Bi AS, Kane LT, Butler BA, Stover MD. Outcomes following extra-articular fractures of the scapula: a systematic review. Injury 2020;51:602–10.
4. Lin TL, Li YF, Hsu CJ, Hung CH, Lin CC, Fong YC, Hsu HC, Tsai CH. Clinical outcome and radiographic change of ipsilateral scapular neck and clavicular shaft fracture: comparison of operation and conservative treatment. J Orthop Surg Res 2015;10:9.
5. Romero J, Schai P, Imhoff AB. Scapular neck fracture–the influence of permanent malalignment of the glenoid neck on clinical outcome. Arch Orthop Trauma Surg 2001;121:313–6.
6. Cole PA, Gauger EM, Herrera DA, Anavian J, Tarkin IS. Radiographic follow-up of 84 operatively treated scapula neck and body fractures. Injury 2012;43:327–33.
7. Bozkurt M, Can F, Kırdemir V, Erden Z, Demirkale İ, Başbozkurt M. Conservative treatment of scapular neck fracture: the effect of stability and glenopolar angle on clinical outcome. Injury 2005;36:1176–81.
8. Bestard EA, Schvene HR, Bestard EH. Glenoplasty in the management of recurrent shoulder dislocation. Contemporary Orthopaedics 1986;12:47–55.
9. Labler L, Platz A, Weishaupt D, Trentz O. Clinical and functional results after floating shoulder injuries. J Trauma 2004;57:595–602.
10. Kim KC, Rhee KJ, Shin HD, Yang JY. Can the glenopolar angle be used to predict outcome and treatment of the floating shoulder? J Trauma 2008;64:174–8.
11. Piyawinijwong S, Sirisathira N, Chuncharunee A. The scapula: osseous dimensions and gender dimorphism in Thais. Siriraj Medical Journal 2004;56:356–65.
12. Sanga A. Role of different angles of scapula: its kinesiometrics muscle morphology and clinical significance. Journal of Medical Science and Clinical Research 2018;6:691–8.
13. Zhang L, Guo X, Liu Y, Ou M, Lin X, Qi J, Xu Y, Wang G, Fu S. Classification of the superior angle of the scapula and its correlation with the suprascapular notch: a study on 303 scapulas. Surg Radiol Anat 2019;41:377–83.
14. Boyan N, Ozsahin E, Kizilkanat E, Soames RW, Oguz O. Assessment of scapular morphometry. Int J Morphol 2018;36:1305–9.
15. Pazarcı Ö, Aytekin N, Kılınç S, Öztürk H. Scapular glenopolar angle in shoulder dislocation cases. Anatomy 2018;12:124–7.
16. Cini NT, Sak NG, Babacan S, Arı İ. Investigation of morphological and biomechanical properties of the scapula for shoulder joint. Medeniyet Medical Journal 2023;38:159–66.
17. Kumari N, Subhash A, Panchal P. Morphometric analysis of glenopolar angle of the scapula in Indian population. Cureus 2024;16:e65189.
18. Pace AM, Stuart R, Brownlow H. Outcome of glenoid neck fractures. J Shoulder Elbow Surg 2005;14:585–90.
19. Tuček M, Naňka O, Malík J, Bartoníček J. The scapular glenopolar angle: standard values and side differences. Skeletal Radiol 2014;43:1583–7.
20. Landin D, Thompson M, Jackson MR. Actions of the biceps brachii at the shoulder: a review. J Clin Med Res 2017;8:667–70.

ORCID ID:
S. Sertel Meyvacı 0000-0002-9450-145X;
H. Ankaralı 0000-0002-3613-0523;
B. Çelik 0000-0003-4401-8678

Correspondence to: Beyza Çelik, PhD
Department of Anatomy, Faculty of Medicine,
Bolu Abant İzzet Baysal University, Bolu, Türkiye
Phone: +90 374 253 46 56
e-mail: beyzayilmazcelik1@gmail.com

deomed

Conflict of interest statement: No conflicts declared.

anatomy
http://dergipark.org.tr/en/pub/anatomy
An International Journal of Experimental and Clinical Anatomy

Review

http://dergipark.org.tr/en/pub/anatomy
Received: August 27, 2024; Accepted: November 28, 2024
doi:10.2399/ana.24.1539427

The locus coeruleus in aging and neurodegenerative diseases

Gülşen Deren Yaman[1], Esra Candar[2], İbrahim Demirçubuk[3], Gülgün Şengül[1]

[1]*Department of Anatomy, School of Medicine, Ege University, Izmir, Türkiye*
[2]*Deparment of Neuroscience, Institute of Health Sciences, Ege University, Izmir, Türkiye*
[3]*Department of Anatomy, Institute of Health Sciences, Ege University, Izmir, Türkiye*

Abstract

The locus coeruleus (LC), a prominent neuromelanin-containing nucleus, plays a critical role in the central nervous system by serving as the main source of norepinephrine. First described by Félix Vicq d'Azyr in the 18th century and later identified as a noradrenaline-rich region through fluorescence histochemistry in the 1960s, the LC influences various brain functions, including attention, learning, stress responses, pain modulation, memory, and sleep. This review explores the anatomy, morphology, and neurochemistry of LC neurons, emphasizing their projections and interactions with multiple brain regions such as the cortex, hippocampus, and thalamus. Additionally, we examine the involvement of the LC in the pathophysiology of age-related neurodegenerative diseases, including Alzheimer's and Parkinson's diseases, where significant neuronal loss in the LC correlates with cognitive decline and other clinical symptoms. Understanding the anatomical and functional heterogeneity of LC neurons provides insights into their crucial role in neuromodulation and highlights potential therapeutic targets for neurodegenerative disorders.

Keywords: brainstem; locus coeruleus; neurodegenerative diseases; norepinephrine

Anatomy 2024;18(3):106–110

Introduction

The locus coeruleus (LC) (**Figure 1**), often referred to as the "blue spot" due to its neuromelanin content, is a distinct structure visible to the naked eye because of its size and pigmentation. Initially described by the French anatomist Félix Vicq d'Azyr in the late 18th century, the LC's primary composition of monoaminergic neurons was not identified until the development of fluorescence histochemistry in the 1960s.[1] The LC, designated as A6 in the classification by Dahlström and Fuxe, is part of the noradrenergic cell groups extending rostrocaudally from the lateral pons to the caudal ventrolateral medulla, as described by these researchers in 1964.[2] As the principal source of norepinephrine in the central nervous system, the LC projects to numerous brain regions, including the cortex, hippocampus, and thalamus, thereby influencing a wide array of functions such as attention, learning, autonomic and behavioral stress responses, pain modulation, memory, and sleep.[3,4] This review focuses on the LC's anatomy, neuronal morphology and neurochemistry, and its significance in neurodegenerative diseases like Alzheimer's and Parkinson's.

Morphology and Neurochemistry

Mature LC neurons are predominantly medium-sized cells with fusiform and multipolar morphologies and sparse branching. The axons of these neurons, especially those extending to the forebrain, exhibit bifurcations that allow them to innervate multiple regions along the neuroaxis of a single neuron. In humans, LC neurons can be classified into four types based on size and dendritic branching: large multipolar neurons, large elliptical "bipolar" neurons, small multipolar neurons, and small ovoid "bipolar" neurons. Large multipolar neurons have round or multiangular somata with numerous thinly branching dendrites that extend in various directions, enabling them to travel long distances and reach different levels. Large bipolar neurons, similar in size to large multipolar neurons, have dendrites emerging as relatively thicker roots from the soma. Small multipolar neurons

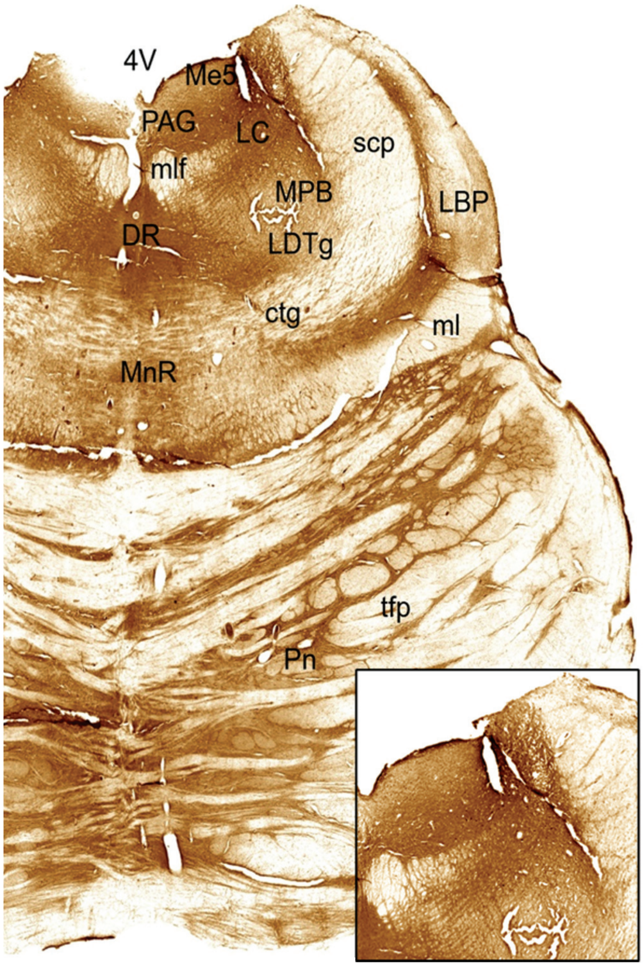

Figure 1. Locus coeruleus localization in the mid-level human pons. **4V**: 4th ventricle; **ctg**: central tegmental tract; **DR**: dorsal raphe nucleus; **LBP**: lateral parabrachial nucleus; **LC**: locus coeruleus; **LDTg**: laterodorsal tegmental nucleus; **Me5**: mesencephalic trigeminal nucleus; **ml**: medial lemniscus; **mlf**: medial longitudinal fasciculus; **MnR**: median raphe nucleus; **MPB**: medial parabrachial nucleus; **PAG**: periaqueductal gray; **Pn**: pontine nuclei; **scp**: superior cerebellar peduncle; **tfp**: transverse fibers of the pons (Unpublished data).

possess round and multiangular somata with dendritic branches arising from all over, but these branches are generally shorter than those of larger neurons. Small bipolar neurons have oval and spindle-shaped somata with dendrites primarily arising from two poles.[5–7]

Besides containing norepinephrine, LC neurons exhibit additional properties that contribute to their diversity. Consistent with their noradrenergic phenotype, LC neurons include the enzymes tyrosine hydroxylase and dopamine beta-hydroxylase involved in norepinephrine production, the norepinephrine transporter,[8] the catabolic enzyme monoamine oxidase,[9] and the α2-adrenoreceptor, which likely functions as an autoreceptor.[10] Furthermore, LC neurons secrete various neuropeptides, including neuropeptide Y,[11] galanin,[12] cholecystokinin, dynorphin A, angiotensin II,[13] and somatostatin.[14]

Anatomy and Projections

The locus coeruleus is situated in the dorsal part of the rostral pons, located in the lateral floor of the fourth ventricle.[15] In a healthy human brain, this nucleus measures about 12 to 17 mm in length and approximately 2.5 mm in width.[16] It is estimated that the bilateral LC neurons in an adult human brain comprise around 45,000 to 50,000 cells.[17]

Understanding the properties of the afferent inputs to the locus coeruleus (LC) is crucial for comprehending the effects of the noradrenergic system on the brain and behavior.[18] The LC is extensively innervated by various nuclei, including the insular cortex, central nucleus of the amygdala, spinal cord dorsal horn and lamina X, ventral tegmental area (VTA), and nucleus of the solitary tract (NST), bed nucleus of the stria terminalis, preoptic region, periaqueductal gray, midbrain pontine reticular formation including the dorsal raphe nucleus, pedunculopontine tegmental nucleus, and cerebellum. LC also receives inputs from area C1 of the ventrolateral medulla[19] and is connected to the dorsal raphe nucleus. Connections to the ventromedial pericoerulear region reported may provide a local circuit interface to LC neurons.[15,19–22] Forebrain afferents include glutamatergic inputs from the prefrontal and anterior cingulate cortices[23] as well as the paragigantocellular nucleus, and perifascicular area of the prepositus hypoglossal nucleus.[21,24] LC neurons receive several afferent inputs and express a wide range of neurotransmitter receptors, indicating multiple levels of cellular regulation. Key neuropeptides include corticotropin-releasing factor, orexin, endogenous opioids, substance P, melanin-concentrating hormone, neuropeptide Y, and somatostatin.[23,25] These neuropeptides regulate LC activity and noradrenaline release, thereby affecting arousal states and related behaviors.[25] Social stress activates specific afferents like CRF from the central amygdalar nucleus and enkephalin from the paragigantocellular nucleus, depending on the individual's coping strategy, with distinct afferents being engaged during short-latency (SL) and long-latency (LL) defeat responses.[26] The LC also receives cholinergic inputs from the basal forebrain, particularly the medial septum, which modulate long-term potentiation (LTP) in the dentate gyrus via noradrenergic pathways, emphasizing a functional loop involving cholinergic and noradrenergic interactions.[27] Additionally, the LC plays a pivotal role in pain modulation and stress-related disorders, influencing pain perception and emotional responses through its connections with the spinal cord, prefrontal cortex, and amygdala.[27,28] These various afferents to the LC underscore its central role in integrating physiological and emotional signals to regulate arousal, stress responses, and cognitive functions.

Sensory signal-processing regions of the brain receive dense innervation from LC.[29] Although LC neurons have sparse dendritic branches, their axons exhibit wide bifurcations, enabling stimulation of many cortical areas.[30] The efferent innervation from the LC includes the cortex, cerebellum, hippocampus, hypothalamus, and spinal cord.[31] This innervation is particularly concentrated in the thalamus, affecting midline, intralaminar, and mediodorsal thalamic nuclei, as well as the lateral posterior complex, periventricular, anteroventral, ventral posterolateral, and reticular nuclei.[32,33] Additionally, the paraventricular and supraoptic nuclei of the hypothalamus are significant targets for LC innervation.[34] Stimulation of LC increases the pupil diameter, indicating LC projections to the parasympathetic Edinger-Westphal nucleus.[22] The LC also projects to the amygdala and medial prefrontal cortex (mPFC), influencing learning and memory functions.[35] Specifically, amygdala-projecting cells are recruited during emotional associative learning, while mPFC-projecting cells are engaged in unexpected situations or when behavioral flexibility is required. Understanding the anatomical and functional heterogeneity of LC neurons is crucial for appreciating their role in the neuromodulatory system.

Involvement in the Pathophysiology of Age-related Neurodegenerative Diseases

The number of neurons in the locus coeruleus (LC) decreases by approximately 30–50% during aging.[5,36,37] This neuronal loss, particularly in those projecting to the forebrain, is linked to functions in arousal, attention, and memory. Several neurodegenerative diseases are associated with age-related LC neuronal loss, including Alzheimer's disease (AD), Down syndrome, Parkinson's disease (PD), dementia with Lewy bodies, progressive supranuclear palsy, corticobasal degeneration, and dementia pugilistica.[38–41] In AD and PD, there can be up to an 80% loss of noradrenergic cells, a reduction greater than the loss of cholinergic neurons in the basal nucleus in AD and dopaminergic neurons in the substantia nigra in PD.[42] Stereological evaluations indicate that in AD, neuronal decline follows a rostrocaudal and dorsoventral pattern, whereas in PD, the loss is concentrated in the more ventral and caudal parts of the LC.[43] Thus, in AD, the LC neuronal loss primarily affects forebrain projections, whereas in PD, the loss impacts spinal cord, brainstem, and cerebellar projections. The reduction in LC neurons is more closely related to the onset and progression of AD than the degeneration of cholinergic neurons in the basal nucleus.[43–45] Recent studies highlight the significance of LC degeneration in the early stages of AD, suggesting that therapies targeting the LC-norepinephrine pathway could be promising for prognosis and treatment, potentially delaying or preventing AD-related pathology.

Conclusion

The LC, a small nucleus with extensive subcortical and cortical projections, is the primary source of norepinephrine innervation in the central nervous system. Due to its broad interaction with various brain regions, the LC significantly influences attention and memory functions in both human and non-human primate brains. In the context of aging and neurodegenerative diseases, the loss of LC neurons can disrupt the integration of sensory, attentional, and cognitive information, leading to age-related memory decline and contributing to the clinical symptoms of various neurodegenerative conditions. Advances in imaging techniques that can visualize the distribution of LC neurons hold promise for future research on the effects of aging and neurodegenerative diseases.

Acknowledgements

We thank the Council of Higher Education of Türkiye for supporting Esra Candar under the 100/2000 CoHE Ph.D. Scholarship Program in the field of “Translational Medicine”.

Conflict of Interest

No conflict of interest was declared by the authors.

Author Contributions

GDY: Conceptualization, manuscript writing - original draft. EC: manuscript writing original draft. İD: manuscript writing - original draft. GŞ: onceptualization, supervision, writing, review and editing.

Ethics Approval

No ethical approval was necessary for this review article.

Funding

The authors reported there is no funding associated with the work featured in this article.

References

1. Carlsson A, Falck B, Hillarp NA. Cellular localization of brain monoamines. Acta Physiol Scand Suppl 1962;56:1–28.
2. Glowinski J, Iversen LL. Regional studies of catecholamines in the rat brain. I. The disposition of [3H]norepinephrin, [3H]dopamine and [3H]dopa in various regions of the brain. Neurochem 1966;13: 655–69.
3. Dahlström A, Fuxe K. Localization of monoamines in the lower brain stem. Experientia 1964;20:398–9.
4. Pertovaara A. Noradrenergic pain modulation. Prog Neurobiol 2006; 80:53–83.
5. Chan-Palay V, Asan E. Quantitation of catecholamine neurons in the locus coeruleus in human brains of normal young and older adults and in depression. J Comp Neurol 1989;287:357–72.
6. Patt S, Gerhard L. A Golgi study of human locus coeruleus in normal brains and in Parkinson's disease. Neuropathol Appl Neurobiol 1993;19:519–23.
7. Arendt T, Schindler C, Brückner MK, Eschrich K, Bigl V, Zedlick D, Marcova L. Plastic neuronal remodeling is impaired in patients with Alzheimer's disease carrying apolipoprotein epsilon 4 allele. J Neurosci 1997;17:516–29.
8. Ordway GA, Stockmeier CA, Cason GW, Klimek V. Pharmacology and distribution of norepinephrine transporters in the human locus coeruleus and raphe nuclei. J Neurosci 1997;17:1710–9.
9. Westlund KN, Denney RM, Kochersperger LM, Rose RM, Abell CW. Distinct monoamine oxidase A and B populations in primate brain. Science 1985;230:181–3.
10. Probst A, Cortés R, Palacios JM. Distribution of alpha 2-adrenergic receptors in the human brainstem: an autoradiographic study using [3H]p-aminoclonidine. Eur J Pharmacol 1984;106:477–88.
11. Chronwall BM, DiMaggio DA, Massari VJ, Pickel VM, Ruggiero DA, O'Donohue TL. The anatomy of neuropeptide-Y-containing neurons in rat brain. Neuroscience 1985;15:1159–81.
12. Ch'ng JL, Christofides ND, Anand P, Gibson SJ, Allen YS, Su HC, Tatemoto K, Morrison JF, Polak JM, Bloom SR. Distribution of galanin immunoreactivity in the central nervous system and the responses of galanin-containing neuronal pathways to injury. Neuroscience 1985;16:343–54.
13. Fodor M, Görcs TJ, Palkovits M. Immunohistochemical study on the distribution of neuropeptides within the pontine tegmentum--particularly the parabrachial nuclei and the locus coeruleus of the human brain. Neuroscience 1992;46:891–908. Erratum in: Neuroscience 1992;48:753.
14. Cooper PE, Fernstrom MH, Rorstad OP, Leeman SE, Martin JB. The regional distribution of somatostatin, substance P and neurotensin in human brain. Brain Res 1981;218:219–32.
15. Counts SE, Mufson EJ. Locus coeruleus. In: Mai JK, Paxinos G, editors. The human nervous system. 3rd ed. Philadelphia (PA): Elsevier Academic Press; 2012. p. 425–7.
16. Fernandes P, Regala J, Correia F, Gonçalves-Ferreira AJ. The human locus coeruleus 3-D stereotactic anatomy. Surg Radiol Anat 2012;34:879–85.
17. Sharma Y, Xu T, Graf WM, Fobbs A, Sherwood CC, Hof PR, Allman JM, Manaye KF. Comparative anatomy of the locus coeruleus in humans and nonhuman primates. J Comp Neurol 2010; 518:963–71.
18. Aston-Jones G, Ennis M, Pieribone VA, Nickell WT, Shipley MT. The brain nucleus locus coeruleus: restricted afferent control of a broad efferent network. Science 1986;234:734–7.
19. Holloway BB, Stornetta RL, Bochorishvili G, Erisir A, Viar KE, Guyenet PG. Monosynaptic glutamatergic activation of locus coeruleus and other lower brainstem noradrenergic neurons by the C1 cells in mice. J Neurosci 2013;33:18792–805.
20. Kim MA, Lee HS, Lee BY, Waterhouse BD. Reciprocal connections between subdivisions of the dorsal raphe and the nuclear core of the locus coeruleus in the rat. Brain Res 2004;1026:56–67.
21. Aston-Jones G, Shipley MT, Chouvet G, Ennis M, van Bockstaele E, Pieribone V, Shiekhattar R, Akaoka H, Drolet G, Astier B, et al. Afferent regulation of locus coeruleus neurons: anatomy, physiology and pharmacology. Prog Brain Res 1991;88:47–75.
22. Saper CB, Stornetta RL. Central autonomic system. In: Paxinos G, editor. The rat nervous system. 4rd ed. San Diego (CA): Elsevier Academic Press; 2015. p. 629–73.
23. Arnsten AF, Goldman-Rakic PS. Selective prefrontal cortical projections to the region of the locus coeruleus and raphe nuclei in the rhesus monkey. Brain Res 1984;306:9–18.
24. Valentino RJ, Page M, Van Bockstaele E, Aston-Jones G. Corticotropin-releasing factor innervation of the locus coeruleus region: distribution of fibers and sources of input. Neuroscience 1992;48:689–705.
25. Zitnik GA. Control of arousal through neuropeptide afferents of the locus coeruleus. Brain Res 2016;1641:338–50.
26. Reyes BA, Zitnik G, Foster C, Van Bockstaele EJ, Valentino RJ. Social stress engages neurochemically-distinct afferents to the rat locus coeruleus depending on coping strategy. eNeuro 2015;2: ENEURO.0042-15.2015.
27. Bergado JA, Frey S, López J, Almaguer-Melian W, Frey JU. Cholinergic afferents to the locus coeruleus and noradrenergic afferents to the medial septum mediate LTP-reinforcement in the dentate gyrus by stimulation of the amygdala. Neurobiol Learn Mem 2007;88:331–41.
28. Suárez-Pereira I, Llorca-Torralba M, Bravo L, Camarena-Delgado C, Soriano-Mas C, Berrocoso E. The role of the locus coeruleus in pain and associated stress-related disorders. Biol Psychiatry 2022;91:786–97.
29. Waterhouse BD, Devilbiss D, Fleischer D, Sessler FM, Simpson KL. New perspectives on the functional organization and postsynaptic influences of the locus ceruleus efferent projection system. Adv Pharmacol 1998;42:749–54.
30. Foote SL, Morrison JH. Extrathalamic modulation of cortical function. Annu Rev Neurosci 1987;10:67–95.

31. Loughlin SE, Foote SL, Bloom FE. Efferent projections of nucleus locus coeruleus: topographic organization of cells of origin demonstrated by three-dimensional reconstruction. Neuroscience 1986;18: 291–306.
32. Morrison JH, Foote SL. Noradrenergic and serotoninergic innervation of cortical, thalamic, and tectal visual structures in old and new world monkeys. J Comp Neurol 1986;243:117–38.
33. Vogt BA, Hof PR, Friedman DP, Sikes RW, Vogt LJ. Norepinephrinergic afferents and cytology of the macaque monkey midline, mediodorsal, and intralaminar thalamic nuclei. Brain Struct Funct 2008;212:465–79.
34. Ginsberg SD, Hof PR, Young WG, Morrison JH. Noradrenergic innervation of the hypothalamus of rhesus monkeys: distribution of dopamine-beta-hydroxylase immunoreactive fibers and quantitative analysis of varicosities in the paraventricular nucleus. J Comp Neurol 1993;327:597–611.
35. Arnsten AF. Stress signalling pathways that impair prefrontal cortex structure and function. Nat Rev Neurosci 2009;10:410–22.
36. Marcyniuk B, Mann DM, Yates PO. The topography of nerve cell loss from the locus caeruleus in elderly persons. Neurobiol Aging 1989;10:5–9.
37. Manaye KF, McIntire DD, Mann DM, German DC. Locus coeruleus cell loss in the aging human brain: a non-random process. J Comp Neurol 1995;358:79–87.
38. Bondareff W, Mountjoy CQ, Roth M. Selective loss of neurones of origin of adrenergic projection to cerebral cortex (nucleus locus coeruleus) in senile dementia. Lancet 1981;1:783–4.
39. Mann DM, Yates PO, Hawkes J. The pathology of the human locus ceruleus. Clin Neuropathol 1983;2:1–7.
40. Gibb WR, Luthert PJ, Marsden CD. Corticobasal degeneration. Brain 1989;112:1171–92.
41. Kosaka K. Dementia and neuropathology in Lewy body disease. Adv Neurol 1993;60:456–63.
42. Zarow C, Lyness SA, Mortimer JA, Chui HC. Neuronal loss is greater in the locus coeruleus than nucleus basalis and substantia nigra in Alzheimer and Parkinson diseases. Arch Neurol 2003;60: 337–41.
43. German DC, Manaye KF, White CL 3rd, Woodward DJ, McIntire DD, Smith WK, Kalaria RN, Mann DM. Disease-specific patterns of locus coeruleus cell loss. Ann Neurol 1992;32:667–76.
44. Mann DM, Yates PO, Marcyniuk B. A comparison of changes in the nucleus basalis and locus coeruleus in Alzheimer's disease. J Neurol Neurosurg Psychiatry 1984;47:201–3.
45. Förstl H, Levy R, Burns A, Luthert P, Cairns N. Disproportionate loss of noradrenergic and cholinergic neurons as cause of depression in Alzheimer's disease-a hypothesis. Pharmacopsychiatry 1994;27: 11–5.

ORCID ID:
G. D. Yaman 0009-0001-6638-3505;
E. Candar 0000-0001-5408-5570;
İ. Demircubuk 0000-0002-6574-9587;
G. Şengul 0000-0002-5826-7379

deomed

Correspondence to: Gülgün Şengül, MD, Prof.
Department of Anatomy, School of Medicine, Ege University,
Bornova, 35100, İzmir, Türkiye
Phone: +90 532 686 09 21
e-mail: gulgun.sengul@ege.edu.tr

Conflict of interest statement: No conflicts declared.

 How to cite this article: Yaman GD, Candar E, Demirçubuk İ, Şengül G. The locus coeruleus in aging and neurodegenerative diseases. Anatomy 2024;18(3):106–110.

Case Report

http://dergipark.org.tr/en/pub/anatomy
Received: September 4, 2024; Accepted: December 12, 2024
doi:10.2399/ana.24.1543458

Unilateral separation of the hypoglossal nerve from the cranial cavity through two hypoglossal foramina: case report

Yusuf Seçgin , Nesibe Yılmaz

Department of Anatomy, Faculty of Medicine, Karabük University, Karabük, Türkiye

Abstract

The twelfth cranial nerve, known as the hypoglossal nerve, is a somatomotor nerve. Functionally, it innervates the intrinsic muscles of the tongue and all extrinsic tongue muscles except the palatoglossus. Anatomically, the hypoglossal nerve exits the cranium via the hypoglossal canal. This case report describes a variation identified during routine dissection of two adult cadavers in the dissection laboratory of the Karabük University Faculty of Medicine, Department of Anatomy. During the standard dissection procedure, the cranial cavity was first exposed, and the brain tissue was removed. Subsequent examination revealed that, in one cadaver, the hypoglossal nerve on the left side exited the cranium through two separate small foramina instead of the typical hypoglossal canal. A review of the literature indicated that reports on this anatomical variation are scarce. This case report aims to contribute valuable insights to the field of anatomy and provide critical information for clinicians performing surgical procedures in this region.

Keywords: anatomical variation; cranial cavity; hypoglossal nerve

Anatomy 2024;18(3):111–113

Introduction

The hypoglossal nerve, also known as the twelfth cranial nerve, is composed exclusively of motor fibers. It innervates all intrinsic and extrinsic muscles of the tongue, with the exception of the palatoglossus muscle. The palatoglossus muscle is innervated by the cranial part of the accessory nerve. The nucleus of the hypoglossal nerve is located in the medulla oblongata (bulb) and is referred to as the hypoglossal nucleus. The nerve exits from the medulla through the hypoglossal canal. It then descends, traversing the carotid and digastric triangles, ultimately reaching and innervating the muscles of the tongue.[1–4]

The morphology of the cranium, along with the structure of its foramina and canals, provides critical insights into human evolution. The hypoglossal canal, situated on the occipital condyle and anterolateral to the foramen magnum, is a significant anatomical feature.[5]

Case Report

This case was identified during routine cranial dissection of cadavers in the dissection hall of the Karabük University Faculty of Medicine, Department of Anatomy. The dissection process involved preparing the cadavers and dissection materials, followed by removing the scalp using a scalpel. The calvaria was then opened with a bone saw, bone-cutting spiral, and osteotome, and the dura mater was carefully dissected. Subsequently, the brain tissue was mobilized and removed to expose the skull base. During the examination of the cranial nerves, it was observed that the hypoglossal nerve on the left side of one cadaver emerged from the anterolateral sulcus as a single root but exited the cranium through two small foramina instead of the typical hypoglossal canal (**Figure 1**). Further dissection of these foramina revealed that they each extended into distinct bony canals (**Figure 2**).

Discussion

The variation anatomy is a crucial branch of anatomical science, focusing on differences that deviate from the typical structure of the human body. This field is built upon extensive anatomical knowledge and the experiences of clinicians performing interventional procedures.

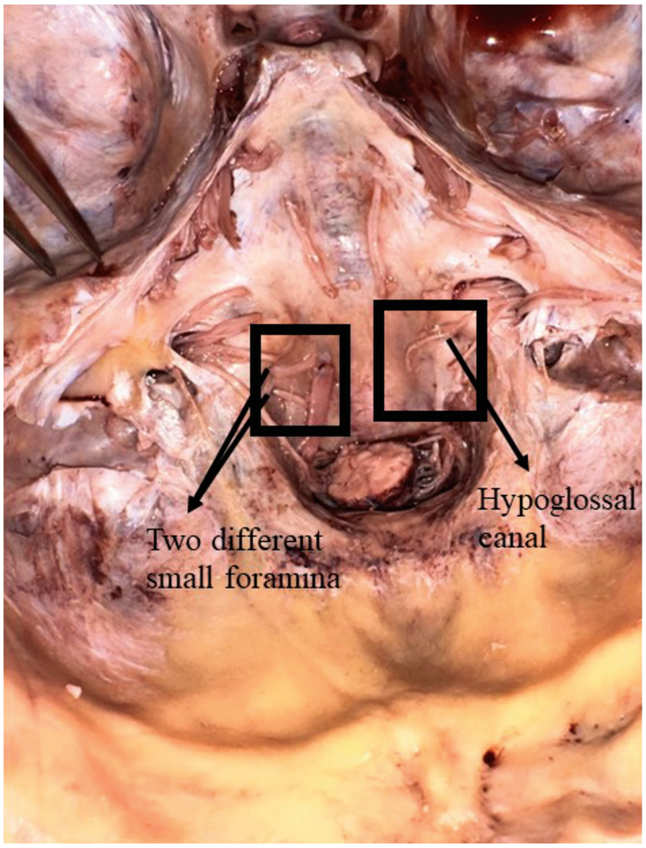

Figure 1. Hypoglossal nerve emerging from two different foramina.

While most anatomical variations do not adversely affect the human body, some can lead to functional impairments or issues involving surrounding tissues. Among anatomical structures, blood vessels exhibit the greatest variability. Regarding nerves, peripheral nerves are the most prone to variation. Variations in the nervous system are significant as they can influence both the nerve's course and its function.[6]

Variations of the hypoglossal nerve most commonly occur in its course after exiting the cranium, with intracranial variations being relatively rare.[1] For instance, Islam et al.[7] reported a case of a 50-year-old male undergoing surgery for facial paralysis, where the hypoglossal nerve was found to give an aberrant branch in the carotid triangle before entering the tongue Bergman et al.[8] described a case where the hypoglossal nerve arose unusually from the posterior aspect of the medulla oblongata.

The hypoglossal canal, an anatomically narrow structure located anterolateral to the foramen magnum, accommodates the hypoglossal nerve, the meningeal branch of the ascending pharyngeal artery, and small vascular plexuses. Its clinical significance stems from its proximity to the occipital lobe and its role in skull base surgeries.[9] Bhuller et al.[10] studied 32 cadavers and reported that the hypoglossal canal was bisected by a small bony fragment in

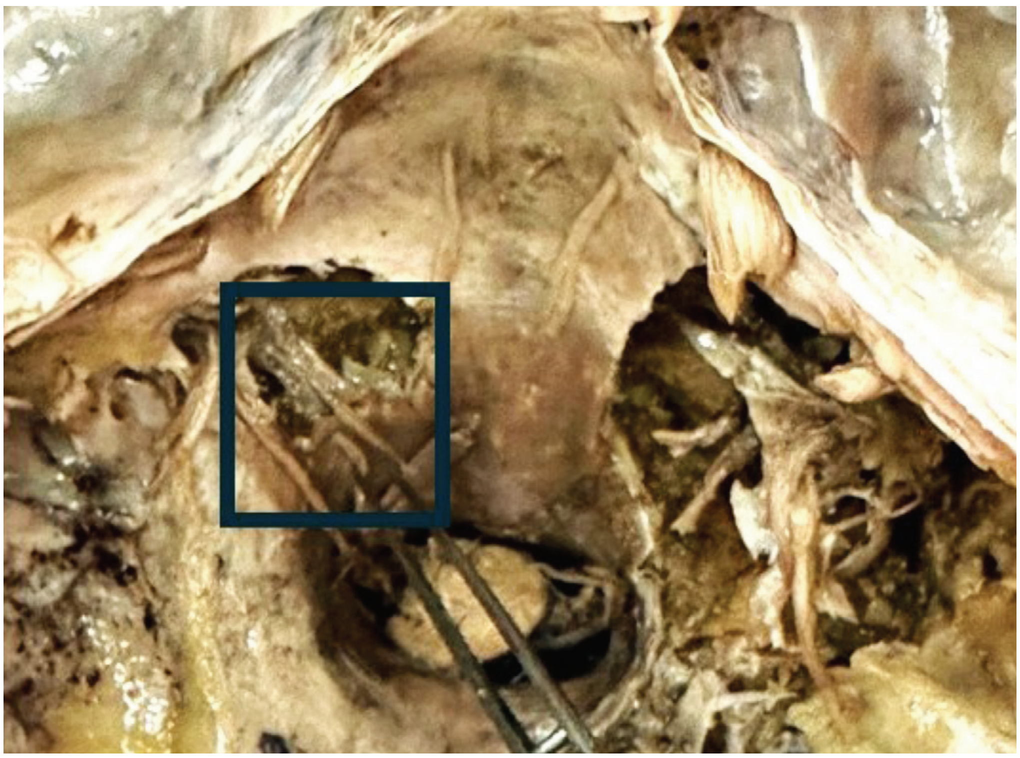

Figure 2. Two separate bony hypoglossal foramina (dissected).

28.12% of cases. Similarly, Wysocki et al.[11] in their study of 100 human skulls and various mammalian skulls, identified double hypoglossal canals in 43% of human skulls. Carolineberry and Bery[12] documented a variation rate of 7–27.4% for the hypoglossal canal in their study on cranial variations. Nikumbh et al.[5] analyzing 100 adult dry skulls, found unilateral hypoglossal canals in 25% of cases and bilateral canals in 3% Zaidi et al. observed double hypoglossal canals in 5 of the 40 dry skulls they studied.[13] Francisco et al.[14] examined 492 human skulls and identified double hypoglossal canals in 97 specimens Muthukumar et al.[15] in a study of 50 dry skulls, noted that the hypoglossal canal was divided into two by a bony septum in 30% of the cases.

In the present case, it was observed that the hypoglossal nerve exited the cranium via two unilateral small foramina instead of the typical hypoglossal canal. It is believed that this finding provides valuable insights for future studies on anatomical variations in cadavers and offers critical guidance for surgeons operating in this region.

Acknowledgements

The authors would like to express their endless gratitude to the body donors and their families who have made great contributions to the science of anatomy.

Conflict of Interest

The authors declare that they have no conflict of interest.

Author Contributions

All authors contributed equally.

Ethics Approval

The authors confirm that they have complied with ethical guidelines for cadaveric studies.

Funding

None.

References

1. Nayak SB. Unilateral, double hypoglossal nerves leaving the cranial cavity through two hypoglossal foramina: a case report. Neuroanatomy 2008;7:6–7.
2. Erzurumlu R, Şengül G, Ulupınar E. Nöroanatomi. Ankara: Güneş Tıp Kitapevleri; 2023. p. 259–60.
3. Yasin A. Her yönüyle anatomi. Istanbul: Istanbul Tıp Kitabevi; 2019. p. 534–6.
4. Arıncı A, Elhan A. Anatomi. 2 cilt. İstanbul: Güneş Kitapevi; 2006. p. 155.
5. Nikumbh RD, Nikumbh DB, Karambelkar RR, Shewale AD. Morphological study of hypoglossal canal and its anatomical variation. International Journal of Health Sciences and Research 2013; 3:54–8.
6. Kachlík D, Varga I, Báča V, Musil V. Variant anatomy and its terminology. Medicina (Kaunas) 2020;56:713.
7. Islam S, Walton G, Howe D. Aberrant anatomy of the hypoglossal nerve. J Laryngol Otol 2012;126:538–40.
8. Bergman R, Thompson S, Afifi A, Saadeh F. Compendium of the human anatomic variation. Text, atlas and world literature. Baltimore (MD): Urban and Schwarzenberg; 1988. p. 200.
9. Demir BT, Patat D. Morphological and morphometric analysis of hypoglossal canal and its importance in cranial base surgery: a skull study. Konuralp Medical Journal 2023;15:136–43.
10. Bhuller A, Sanudo J, Choi D, Abrahams P. Intracranial course and relations of the hypoglossal nerve: an anatomic study. Surg Radiol Anat 1998;20:109–12.
11. Wysocki J, Kobryń H, Bubrowski M, Kwiatkowski J, Reymond J, Skarżyńska B. The morphology of the hypoglossal canal and its size in relation to skull capacity in man and other mammal species. Folia Morphol (Warsz) 2004;63:11–7.
12. Carolineberry A, Berry RJ. Epigenetic variation in the human cranium. J Anat 1967;101:361.
13. Zaidi S, Gupta R, Usman N. A study of hypoglossal canal in north indian crania. Journal of Anatomical Society of India 2011;60:224–6.
14. De Francisco M, Lemos J, Liberti E, Adamo J, Jacomo A, Matson E. Anatomical variations in the hypoglossal canal. Rev Odontol Univ Sao Paulo 1990;4:38–42.
15. Muthukumar N, Swaminathan R, Venkatesh G, Bhanumathy S. A morphometric analysis of the foramen magnum region as it relates to the transcondylar approach. Acta Neurochir (Wien) 2005;147:889–95.

ORCID ID:
Y. Seçgin 0000-0002-0118-6711;
N. Yılmaz 0000-0002-5527-8507

Correspondence to: Yusuf Seçgin, PhD
Department of Anatomy, Faculty of Medicine,
Karabük University, Karabük, Türkiye
Phone: +90 507 784 46 72
e-mail: yusufsecgin@karabuk.edu.tr

deomed

Conflict of interest statement: No conflicts declared.

anatomy
http://dergipark.org.tr/en/pub/anatomy
An International Journal of Experimental and Clinical Anatomy
http://dergipark.org.tr/en/pub/anatomy
Anatomy 2024;18(3):114 ©2024 Turkish Society of Anatomy and Clinical Anatomy (TSACA)

Author Index to Volume 18, 2024

(The bold typed references are the ones in which the person is the first author.)

http://dergipark.org.tr/en/pub/anatomy
Anatomy 2024;18(3):115 ©2024 Turkish Society of Anatomy and Clinical Anatomy (TSACA)

anatomy
http://dergipark.org.tr/en/pub/anatomy
An International Journal of Experimental and Clinical Anatomy

Acknowledgment of Reviewers for Volume 18, 2024

The Editorial Staff of Anatomy expresses their appreciation to the following reviewers who have evaluated the manuscripts for Volume 18, 2024.

Esat Adıgüzel
Hilal Akdemir Aktaş
Mustafa Aldur
Kerem Atalar
Meltem Bahçelioğlu
Aybegüm Balcı
Çağatay Barut
Alev Bobus Örs
Murat Bozkurt
Ayhan Cömert
Ela Cömert
Nurdan Çay
Nadire Ünver Doğan
Burcu Erçakmak Güneş
Zeliha Fazlıoğulları
Ayşegül Fırat
Nermin Nükhet Göçmen Karabekir
Yiğit Güngör
İlke Ali Gürses
David Kachlik
Süleyman Tuna Karahan
Simel Kendir
Zeliha Kurtoğlu Olgunus
Ayla Kürkçüoğlu
Mehmet Ali Malas
Mert Nahir
Hale Öktem
Hilmi Özden
Ahmet Sınav
Muzaffer Sindel
Carla Stecco
Bilge İpek Torun
Trifon Totlis
Selçuk Tunalı
Aysun Uz
Mehmet Üzel
Alper Vatansever
Abdullah Yıldız
Mehmet Yılmaz

Table of Contents

Volume **18** / Issue **3** / December **2024** *(Continued from back cover)*

Review

Case Report

Index

On the Front Cover:
Measurements of length (**a**), width (**b**) and area (**c**) of abductor pollicis brevis. From Adanır SS, Korkmaz S, Beger O, Bahşi İ, Kervancıoğlu P, Orhan M. Fetal anatomy of the abductor pollicis brevis and its clinical importance. *Anatomy* 2024;18(3):73–82.

http://dergipark.org.tr/en/pub/anatomy

anatomy

An International Journal of Experimental and Clinical Anatomy

Table of Contents

Volume **18** / Issue **3** / December **2024**

Original Articles

(Contents continued on inside back cover)

deomed®